Properties of hyperons in nuclear matter with baryon-baryon interactions constructed in chiral effective field theory

Michio Kohno, RCNP Osaka University

- baryon-baryon interactions in chiral effective field theory (ChEFT)
  - Chiral symmetry
  - Construction (parametrization) of baryon-barton interactions
- three-body forces
- ΛN and ΛNN interactions
- Properties of Λ in the nuclear medium (symmetric nuclear matter)
- 3-body forces in hypertriton and Λ-deuteron correlation functions

NN interactions and Three-body forces (induced many-body forces)

- Instantaneous B-B potentials are derived through the elimination of various degrees of freedom, such as mesons and baryon excited states.
  - In principle, by unitary transformation.
  - No problem for on-shell properties in a two-body system.
  - Unitary transformation induces many-body forces in many-baryon systems.

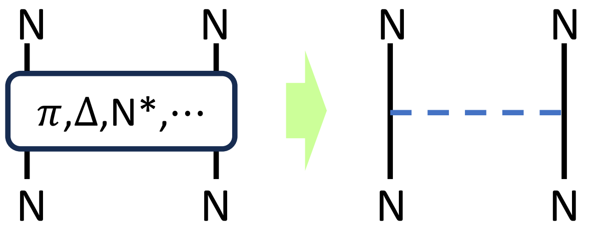

- Low-momentum interactions in model space P.
  - Correlations involving states in Q-space are eliminated.
  - Many-body interactions manifest in model space P.

    (induced three-body interaction)

$\langle k'|H|k\rangle \quad \tilde{H} = e^{-S_{12}}\, H e^{S_{12}} \quad \langle k'|\tilde{H}|k\rangle$

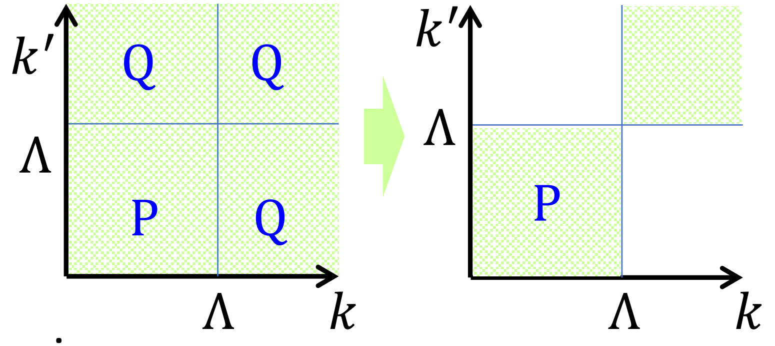

- In ChEFT, the chiral symmetric Lagrangian of nucleons and pions is determined in low-momentum space (power counting). The pions are subsequently eliminated.

Construction of (instantaneous) NN interactions

- Eliminate other degrees of freedom than nucleons by a unitary transformation.

  [Okubo, PTP12 (1954), Taketani-Machida-Ohnuma, PTP7 (1954)]

  [Epelbaum, arXiv:1001.3229 "Nuclear forces from Ch-EFT: a primer"]

$$H = \begin{pmatrix} PHP & PHQ \\ QHP & QHQ \end{pmatrix} \Rightarrow H_{eff} = \tilde{X}^{-1} H \tilde{X}$$

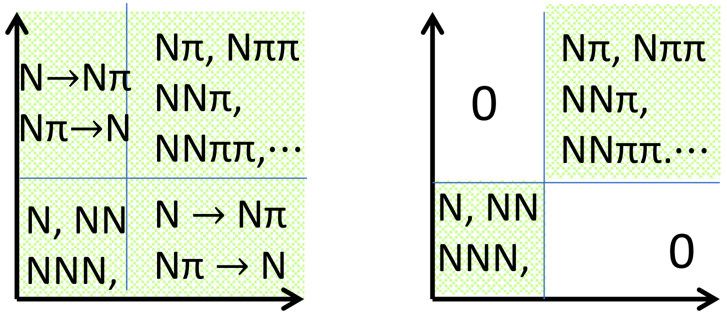

➢ decoupling eq. $QHP + QHQ\omega - \omega PHP - \omega PHQ\omega = 0$ is solved perturbatively. Time-ordered perturbation.

$$V_{eff} = H_{eff} - PHP = -g^2 P\left[\frac{1}{2} H_1 \frac{1}{H_0 - E_Q} H_1 + h.c.\right] P$$
$$-g^4 P\left[\frac{1}{2} H_1 \frac{1}{H_0 - E_Q} H_1 \frac{1}{H_0 - E_Q} H_1 \frac{1}{H_0 - E_Q} H_1 + \cdots\right] P + \cdots$$

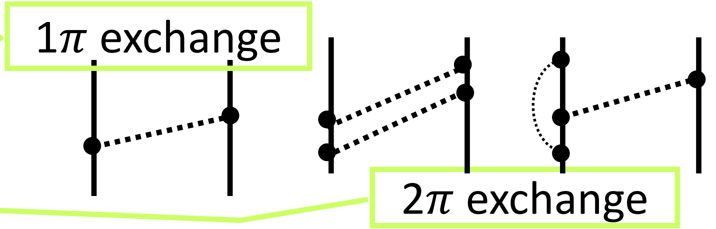

- The unitary transformation induces many-body forces in many-nucleon space.
- Calculations of Feynman diagrams directly provide the Born amplitudes of the corresponding potential.

Chiral symmetry

- Before QCD
  - PCAC: axial-current conservation implies (chiral) symmetry
  - Pion is not chirally invariant. Pion is a Nambu-Goldstone due to the spontaneous breaking of the chiral symmetry. [chiral transformation (ch-x) $e^{i\theta\gamma_5}$]
  - Effective model such as linear σ-model: $(\boldsymbol{\pi}, \sigma)$ where $\boldsymbol{\pi}^2 + \sigma^2$ is invariant under ch-x.
- QCD: $\mathcal{L}_{QCD} = \bar{q}\left(i\gamma^\mu \mathcal{D}_\mu - \mathcal{M}\right)q - \frac{1}{4}\mathcal{G}_{\mu\nu,a}\mathcal{G}_a^{\mu\nu}$, small mass term $\mathcal{M} = \begin{pmatrix} m_u & 0 & 0 \\ 0 & m_d & 0 \\ 0 & 0 & m_s \end{pmatrix}$
  - $\mathcal{L}_{QCD}^0 = \bar{q}i\gamma^\mu \mathcal{D}_\mu q - \frac{1}{4}\mathcal{G}_{\mu\nu,a}\mathcal{G}_a^{\mu\nu} = \bar{q}_R i\gamma^\mu \mathcal{D}_\mu q_R + \bar{q}_L i\gamma^\mu \mathcal{D}_\mu q_L - \frac{1}{4}\mathcal{G}_{\mu\nu,a}\mathcal{G}_a^{\mu\nu}$

    $q = \left[\frac{1}{2}(1+\gamma_5) + \frac{1}{2}(1-\gamma_5)\right] q \equiv q_R + q_L$ (SU$\binom{2}{3}_R \times$ SU$\binom{2}{3}_L$)

$m_u \cong$ 2.5 MeV,
$m_d \cong$ 5 MeV,
$m_s \cong$ 101 MeV

- The proposal by Weinberg (1979): consider an effective model with a general chiral-symmetric Lagrangian instead of specific models.

Chiral-invariant Lagrangian for meson-baryon coupling

- flavor SU(3)×SU(3) : octet baryons and pseudoscalar (ps) mesons

$$(B_{ij}) = \begin{pmatrix} \frac{\Sigma^0}{\sqrt{2}}+\frac{\Lambda}{\sqrt{6}} & \Sigma^+ & p \\ \Sigma^- & -\frac{\Sigma^0}{\sqrt{2}}+\frac{\Lambda}{\sqrt{6}} & n \\ -\Xi^- & \Xi^0 & -\frac{2\Lambda}{\sqrt{6}} \end{pmatrix}, \quad (P_{ij}) = \begin{pmatrix} \frac{\pi^0}{\sqrt{2}}+\frac{\eta}{\sqrt{6}} & \pi^+ & K^+ \\ \pi^- & -\frac{\pi^0}{\sqrt{2}}+\frac{\eta}{\sqrt{6}} & K^0 \\ -K^- & \bar{K}^0 & -\frac{2\eta}{\sqrt{6}} \end{pmatrix}$$

- Meson-Baryon coupling

$$u^2 = exp\left(i\sqrt{2}P/f_0\right)$$

$$D_\mu B = \partial_\mu B + \left[\frac{1}{2}\left(u^\dagger \partial_\mu u + u\partial_\mu u^\dagger\right), B\right], \qquad u_\mu = i\left(u^\dagger \partial_\mu u - u\partial_\mu u^\dagger\right)$$

$$\mathcal{L}_{MBB} = \mathrm{tr}\left(\bar{B}(i\gamma^\mu D_\mu - M_0)B\right) - \frac{D}{2}\mathrm{tr}\left(\bar{B}\gamma^\mu\gamma_5\{u_\mu , B\}_\mu\right) - \frac{F}{2}\mathrm{tr}\left(\bar{B}\gamma^\mu\gamma_5[u_\mu , B]\right)$$

➢ Low-energy effective theory: expansion in terms of *P* and non-relativistic approx.

NN, πNN contact, πNN, and $\pi\pi$NN Lagrangian

- NN and πNN contact terms that describe the physics beyond the cutoff scale.

$$\mathcal{L}_{NN} = -\frac{1}{2}C_S\bar{N}N\bar{N}N - \frac{1}{2}C_T(\bar{N}\boldsymbol{\sigma}N)(\bar{N}\boldsymbol{\sigma}N) - \frac{D}{4f_\pi^2}(\bar{N}N)\bar{N}[\boldsymbol{\tau}\cdot(\boldsymbol{\sigma}\cdot\nabla)\boldsymbol{\pi}]N - \frac{E}{2}(\bar{N}N)(\bar{N}\boldsymbol{\tau}N)\cdot(\bar{N}\boldsymbol{\tau}N)$$

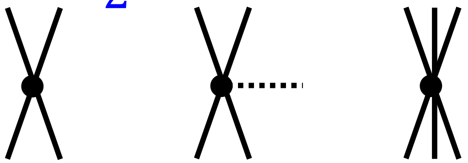

- πNN, and $\pi\pi$NN up to two-derivative terms of the pion field

$$\begin{aligned}\mathcal{L}_{\pi NN} &= \bar{N}\left[i\partial_0 - \frac{g_A}{2f_\pi}\boldsymbol{\tau}\cdot(\boldsymbol{\sigma}\cdot\nabla)\boldsymbol{\pi} - \frac{D}{4f_\pi^2}\boldsymbol{\tau}\cdot(\boldsymbol{\pi}\times\partial_0\boldsymbol{\pi})\right]N \\ &+\bar{N}\left[\frac{1}{2M_N}\nabla^2 - \frac{ig_A}{4M_Nf_\pi}\boldsymbol{\tau}\cdot\left[\boldsymbol{\sigma}\cdot\left(\overleftarrow{\nabla}\partial_0\boldsymbol{\pi} - \partial_0\boldsymbol{\pi}\nabla\right)\right] - \frac{i}{8M_Nf_\pi^2}\boldsymbol{\tau}\cdot[\overleftarrow{\nabla}\cdot(\boldsymbol{\pi}\times\boldsymbol{\nabla}\boldsymbol{\pi}) - (\boldsymbol{\pi}\times\boldsymbol{\nabla}\boldsymbol{\pi})\cdot\nabla]\right]N \\ &+\bar{N}\left[4c_1m_\pi^2 - \frac{2c_1}{f_\pi^2}m_\pi^2\boldsymbol{\pi}^2 + \left(c_2 - \frac{g_A^2}{8M_N}\right)\frac{1}{f_\pi^2}(\partial_0\boldsymbol{\pi}\cdot\boldsymbol{\partial_0\pi})\right. \\ &\qquad\left.+\frac{c_3}{f_\pi^2}(\partial_\mu\boldsymbol{\pi}\cdot\boldsymbol{\partial}^\mu\boldsymbol{\pi}) + \left(c_4 + \frac{1}{4M_N}\right)\frac{1}{2f_\pi^2}\epsilon^{ijk}\epsilon^{abc}\sigma^i\tau^a(\partial^j\pi^b)(\partial^k\pi^c)\right]N\end{aligned}$$

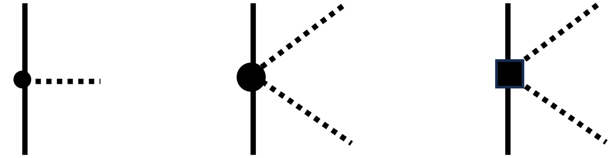

➢ Parameters are fitted by analyzing πN scattering data.

Feynman diagrams in each chiral order ν (power counting)

$\nu = 0$

$\nu = 1$ is absent

$\nu = 2$

$\nu = 3$

$\nu = 4$

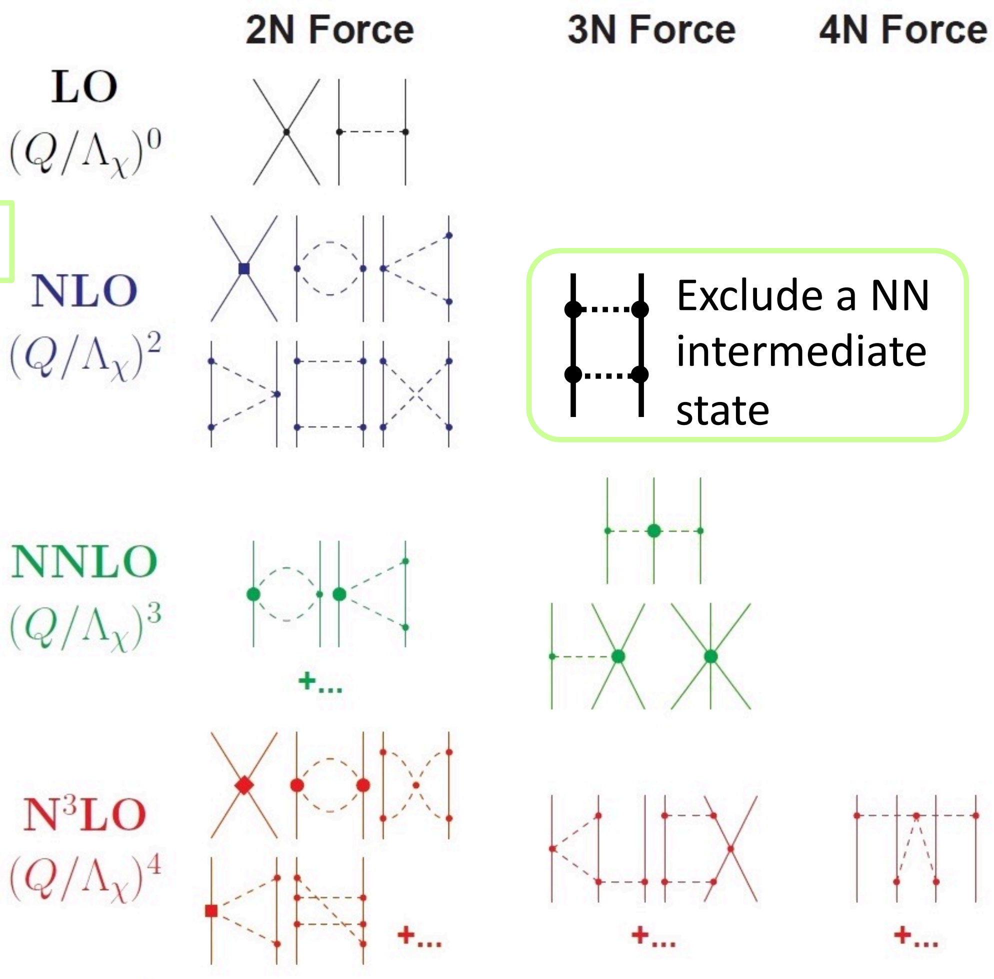

Exclude a NN intermediate state

- N^{2}LO can fit the scattering data well.
  - (N^{5}LO parametrization is present.)
- The number of parameters is about 30 at N^{2}LO.
  - The parametrization that incorporates the Isobar Δ in the Feynman diagrams is also attempted.

Power counting

- The guideline to derive a potential.

  power counting, Weinberg (1979)

  - Feynman diagrams are organized in according to the order ν of the low-momentum Q (low-momentum scale $(Q/\Lambda)^{\nu}$): the expansion in terms of ν

- Diagrams consisting exclusively of nucleons are excluded from consideration. They are included in solving the Lippmann-Schwinger equation after constructing the potential.

  (It is not possible to describe a bound state by perturbation.)

- ν is given by $\nu = 2L + \sum_i (d_i + \frac{n_i}{2} - 2)$, where i specifies a vertex, d_i (n_i) is the number of the derivative at the vertex (nucleons), and L is the number of loops.

  (In the case of 3BF, $\nu = 2 + 2L + \sum_i (d_i + \frac{n_i}{2} - 2)$)

example： next-to-leading order (NLO) $\nu = 2$

- Typical example of $\nu = 2L + \sum_i (d_i + \frac{n_i}{2} - 2) = 2$ diagram

The diagram with 3 vertices ($n_{1,2,3} = 2,\ d_{1,2,3} = 1$) and 1 loop ($L = 1$) corresponds to two-pion exchange.

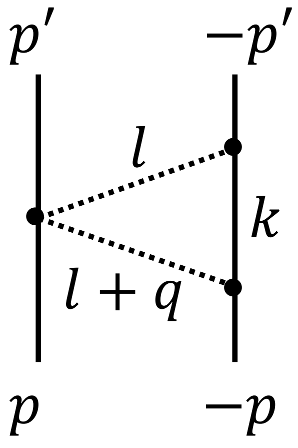

$$V = i\frac{g_A^2}{16f_\pi^4}\int\frac{d^4 l}{(2\pi)^4}(2l^\mu + q^\mu)\epsilon^{abc}\tau_1^c\,\bar{u}_1(\boldsymbol{p}')\gamma_\mu u_1(\boldsymbol{p})\frac{i}{l^2 - m_\pi^2 + i\varepsilon}$$
$$\times\frac{i}{(l+q)^2 - m_\pi^2 + i\varepsilon}\bar{u}_2(-\boldsymbol{p}')(-l^\nu)\tau_2^b\gamma_\nu\gamma_5\frac{i(k\cdot\gamma + M_N)}{k_N^2 - M_N^2 + i\varepsilon}(l^\rho + q^\rho)\tau_2^a\gamma_\rho\gamma_5 u_2(-\boldsymbol{p})$$

$$\Rightarrow\ \boldsymbol{\tau}_1\cdot\boldsymbol{\tau}_2\frac{g_A^2}{(4\pi)^2}\frac{1}{24f_\pi^4}\Bigg[(18m_\pi^2 + 5q^2)\left(-\frac{2}{\eta} + \gamma - 1 - \ln 4\pi\right) - 4m_\pi^2 - \frac{13}{3}q^2$$
$$+(16m_\pi^2 + 10q^2)\frac{\sqrt{q^2 + 4m_\pi^2}}{q}\ln\frac{\sqrt{q^2 + 4m_\pi^2} + q}{2m_\pi} + 2(18m_\pi^2 + 5q^2)\ln\frac{m_\pi}{\lambda}\Bigg]$$

example : next-to-next-to-leading order (NNLO) $\nu = 3$

- Example of $\nu = 3$ two-pion exchange $(L = 1)$ loop diagram

The diagram with one vertex of $n = 2, d = 2$ and two vertices of $n = 2, d = 1$.

(low-energy constants $c_1, c_3,$ and c_4 emerge, which contribute to 3BFs.)

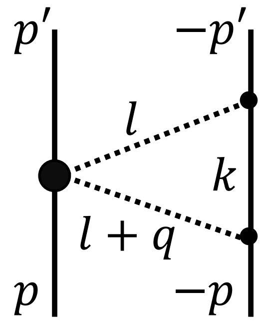

$$\frac{3g_A^2}{16\pi f_\pi^4}\left\{\frac{g_A^2 m_\pi^5}{16M_N(q^2+4m_\pi^2)} - \left[2m_\pi^2(2c_1 - c_3) - q^2\left(c_3 + \frac{3g_A^2}{16M_N}\right)\right]\frac{(q^2+2m_\pi^2)}{2q}\tan^{-1}\frac{q}{2m_\pi}\right\}$$
$$+\boldsymbol{\tau}_1\cdot\boldsymbol{\tau}_2\frac{g_A^2}{128\pi M_N f_\pi^4}\left\{\frac{3g_A^2 m_\pi^5}{q^2+4m_\pi^2} - [4m_\pi^2 + 2q^2 - g_A^2(q^2+4m_\pi^2)]\frac{(q^2+2m_\pi^2)}{2q}\tan^{-1}\frac{q}{2m_\pi}\right\}$$
$$+\frac{\boldsymbol{\sigma}_1\cdot\boldsymbol{\sigma}_2 + S_{12}(\boldsymbol{k})}{3}\left[\frac{9g_A^2}{512\pi M_N f_\pi^4}\frac{(q^2+2m_\pi^2)}{2q}\tan^{-1}\frac{q}{2m_\pi} - \boldsymbol{\tau}_1\cdot\boldsymbol{\tau}_2\frac{3g_A^2}{32\pi f_\pi^4}\left\{\left(c_4 + \frac{1}{4M_N}\right)(q^2+4m_\pi^2) - \frac{g_A^2}{8M_N}(10m_\pi^2\right.\right.$$
$$\left.\left. + 3q^2)\right\}\frac{1}{2q}\tan^{-1}\frac{q}{2m_\pi}\right]$$
$$-i\frac{1}{2}(\boldsymbol{\sigma}_1+\boldsymbol{\sigma}_2)\cdot(\boldsymbol{q}\times\boldsymbol{k})\{\cdots\cdots\cdots\cdots\cdots\}$$

Leading order (NNLO) 3-nucleon forces (explicit expression)

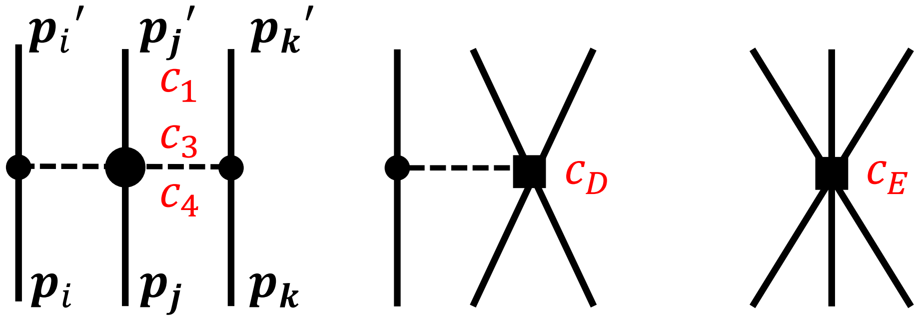

$V_{3N}^{(2\pi)}$ $V_{3N}^{(1\pi)}$ $V_{3N}^{(\mathrm{ct})}$

- $c_1, c_3,$ and c_4 are determined in the two-body sector
- c_D and c_E are new and (usually) fitted in few-body systems.

$\boldsymbol{q}_i = \boldsymbol{p}_i{}' - \boldsymbol{p}_i, \quad \Lambda_\chi = 700$ MeV

$$V_{3N}^{(2\pi)} = \sum_{i \neq j \neq k} \frac{g_A^2}{8 f_\pi^4} \frac{(\boldsymbol{\sigma}_i \cdot \boldsymbol{q}_i)(\boldsymbol{\sigma}_j \cdot \boldsymbol{q}_j)}{(\boldsymbol{q}_i^2 + m_\pi^2)(\boldsymbol{q}_j^2 + m_\pi^2)} F_{ijk}^{\alpha\beta} \tau_i^\alpha \tau_j^\beta$$

$$F_{ijk}^{\alpha\beta} = \delta^{\alpha\beta}\left[-4 c_1 m_\pi^2 + 2 c_3 \boldsymbol{q}_i \cdot \boldsymbol{q}_j\right] + c_4 \epsilon^{\alpha\beta\gamma} \tau_k^\gamma \boldsymbol{\sigma}_k \cdot \left(\boldsymbol{q}_i \times \boldsymbol{q}_j\right)$$

$$V_{3N}^{(1\pi)} = -\sum_{i \neq j \neq k} \frac{g_A c_D}{8 f_\pi^4 \Lambda_\chi} \frac{\boldsymbol{\sigma}_j \cdot \boldsymbol{q}_j}{(\boldsymbol{q}_j^2 + m_\pi^2)} \boldsymbol{\sigma}_i \cdot \boldsymbol{q}_j \boldsymbol{\tau}_i \cdot \boldsymbol{\tau}_j,$$

$$V_{3N}^{(\mathrm{ct})} = \sum_{i \neq j \neq k} \frac{c_E}{2 f_\pi^4 \Lambda_\chi} \boldsymbol{\tau}_i \cdot \boldsymbol{\tau}_j$$

- Subleading-order 3NF's have been worked out beyond N^{2}LO.

3BF contribution in view of Pauli blocking

- Typical 3-BF： Fujita-Miyazawa type Δ-excitation
- Δ-excitation is important in two-body correlations ➡attractive contribution
  - ➢ This effect is implicitly taken care of, when an NN potential is parametrized.

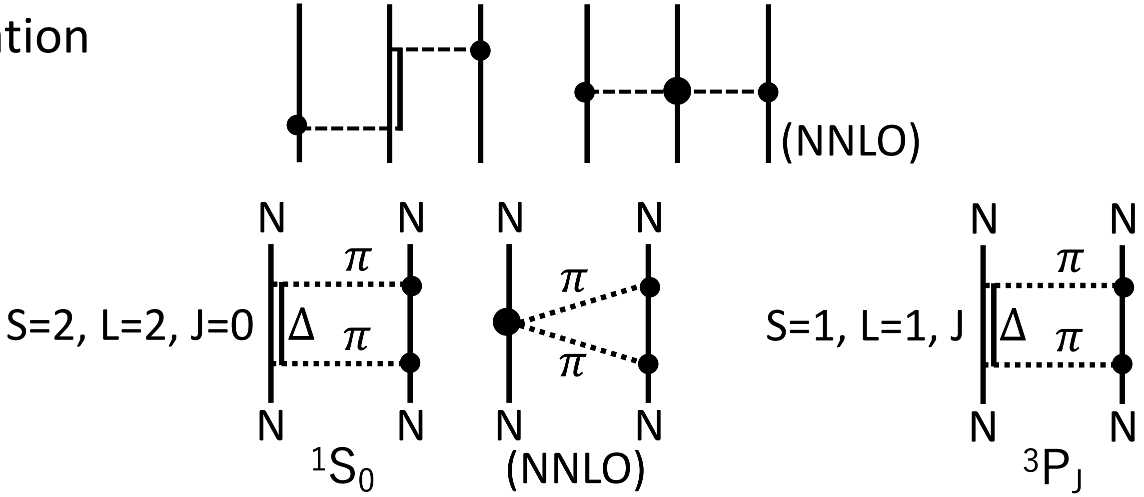

- Δ-excitation is Pauli-blocked (partly) in the nuclear medium, but this effect cannot be treated by the parametrized NN potential.
- The Pauli-blocking effect is taken care of by including 3BFs.

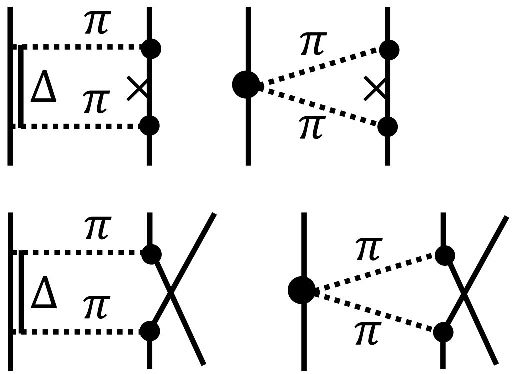

3BF (c1, c2, and c4) contributions to the saturation curve in SNM

- LOBT calculations in symmetric nuclear matter.
  - Nuclear saturation can not be reproduced when only two-body interactions are considered.
  - Calculations using chiral N^3LO interactions.
    - Off-shell properties are different, although on-shell properties are nearly equivalent.
- Contributions of 3BFs (normal-ordered density dependent two-body interactions), their parameters of which are determined in the two-body sector, are repulsive at high densities.
  - To reproduce the empirical saturation point, the values of the contact parameters (c_D and c_E) are adjusted, which may be different from those for light nuclei.

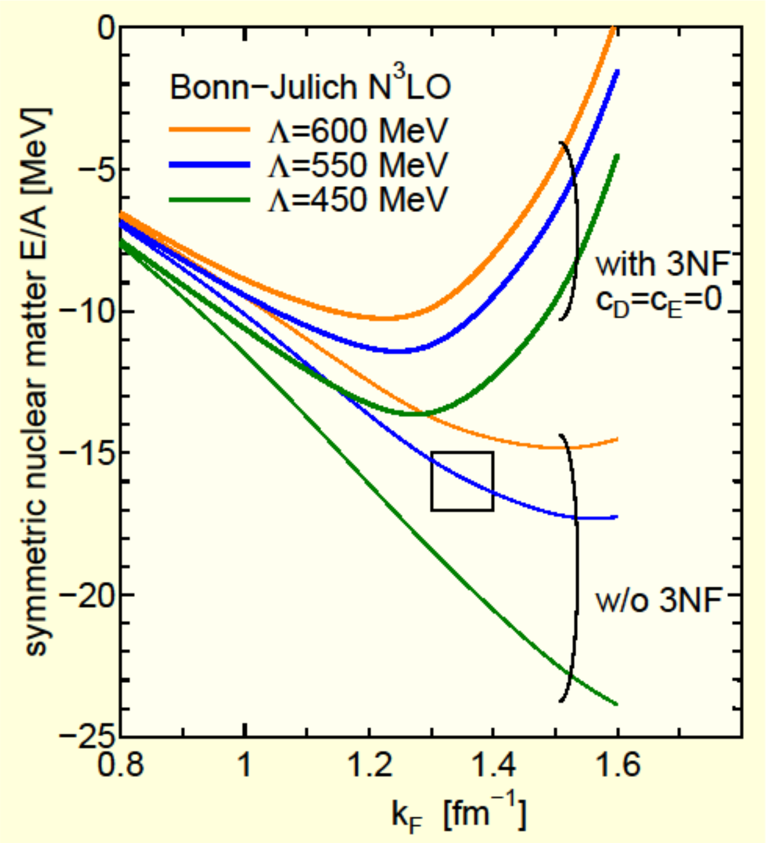

Attractive and repulsive contributions of 3NFs in nuclear matter

- Tensor component in $^3S_1$ is enhanced by 3NFs ➡ attractive contribution in $^3S_1$ channel.
- Δ-excitation processes in $^1S_0$ and ^3P_J channels are Pauli blocked ➡ repulsive contribution.

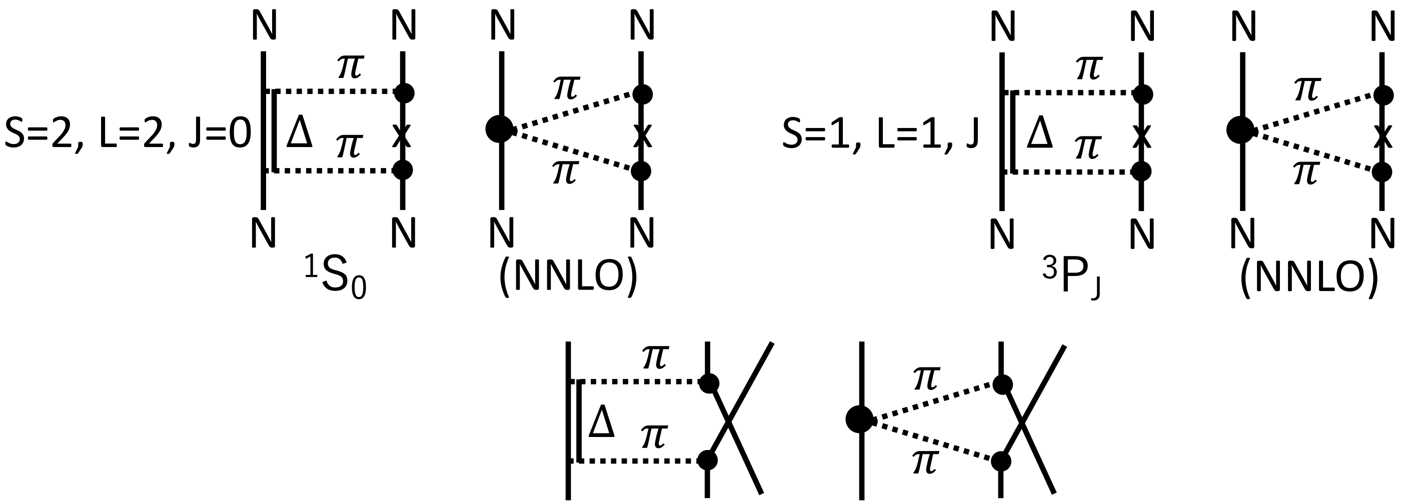

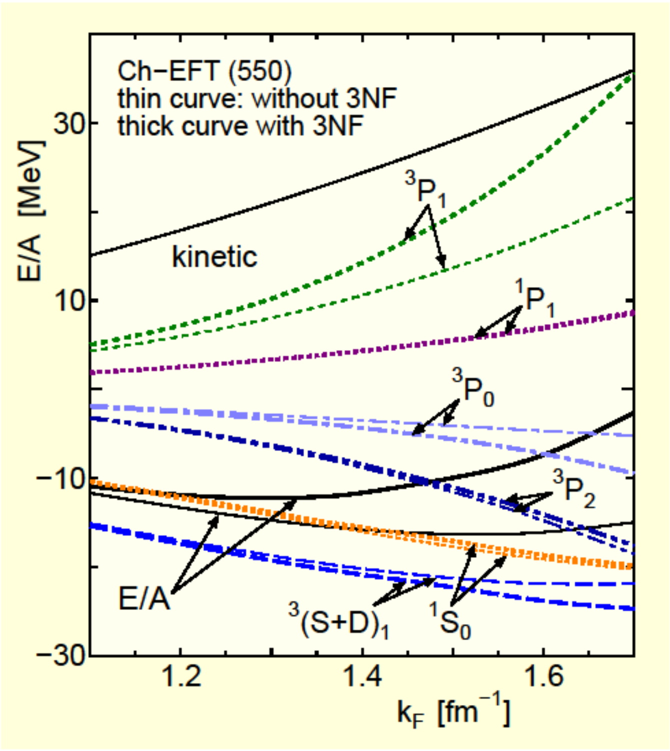

- The repulsive contribution in the ^3P_J channel is large.
- The repulsive contribution in the $^1S_0$ channel is small.

ΛN potentials

- Before 2000: OBEP by Nijmegen group, quark model by Kyoto-Niigata group, and others
  - Advancement of the description of NN interactions in chiral effective field theory
    - Based on the chiral symmetry and its spontaneous breaking pattern
    - Systematic introduction of many-body forces consistent with two-body parameters
    - Possibility of estimating the range of uncertainty
  - ChEFT NN interactions are now standard for studying nuclear structures and reactions
- Parametrization of the interaction of the strangeness sector in ChEFT by Jülich-Bonn- München group
  - NLO13: "Hyperon-nucleon interaction at next-to-leading order in chiral effective field theory,“
    Haidenbauer, Petschauer, Kaiser, Meißner, Nogga, and Weise, Nucl. Phys. A915, 24 (2013).
  - NLO19: “Hyperon-nucleon interaction within chiral effective filed theory revisited”,
    Haidenbauer, Meißner, and Nogga, Eur. Phys. J. A (2020) 56:91.
  - NNLO: "Hyperon-nucleon interaction in chiral effective field theory at next-to-next-to-leading order,“
    Haidenbauer, Meißner, Nogga, and Le, Eur. Phys. J. A (2023) 59:63.
- The parametrization based on Lattice data is not available for quantitative studies.

Leading-order SU$_f$(3) invariant MBB coupling

- Leading-order SU$_f$(3) invariant MBB coupling Lagrangian

$$\mathcal{L}_1 = -\frac{\sqrt{2}}{2f_0}\mathrm{tr}\left(D\bar{B}\gamma^\mu\gamma_5\{\partial_\mu P, B\} + F\bar{B}\gamma^\mu\gamma_5[\partial_\mu P, B]\right)$$

Explicit expression:

$$\begin{aligned}\mathcal{L}_1 = &-f_{NN\pi}\bar{N}\gamma^\mu\gamma_5\boldsymbol{\tau}N\cdot\partial_\mu\boldsymbol{\pi} + if_{\Sigma\Sigma\pi}\bar{\boldsymbol{\Sigma}}\gamma^\mu\gamma_5\times\boldsymbol{\Sigma}\cdot\partial_\mu\boldsymbol{\pi} - f_{\Xi\Xi\pi}\bar{\Xi}\gamma^\mu\gamma_5\boldsymbol{\tau}\Xi\cdot\partial_\mu\boldsymbol{\pi}\\ &-f_{\Lambda\Sigma\pi}[\bar{\Lambda}\gamma^\mu\gamma_5\boldsymbol{\Sigma} + \bar{\boldsymbol{\Sigma}}\gamma^\mu\gamma_5\Lambda]\cdot\partial_\mu\boldsymbol{\pi} - f_{\Lambda NK}[\bar{N}\gamma^\mu\gamma_5\Lambda\partial_\mu K + \bar{\Lambda}\gamma^\mu\gamma_5 N\partial_\mu K^\dagger]\\ &-f_{\Xi\Lambda K}\left[\bar{\Xi}\gamma^\mu\gamma_5\Lambda\partial_\mu\bar{K} + \bar{\Lambda}\gamma^\mu\gamma_5\Xi\partial_\mu\bar{K}^\dagger\right] - f_{\Sigma NK}[\bar{\boldsymbol{\Sigma}}\gamma^\mu\gamma_5\partial_\mu K^\dagger\boldsymbol{\tau}N + \bar{N}\gamma^\mu\gamma_5\boldsymbol{\tau}\partial_\mu K\cdot\boldsymbol{\Sigma}]\\ &-f_{\Xi\Sigma K}\left[\bar{\boldsymbol{\Sigma}}\gamma^\mu\gamma_5\partial_\mu\bar{K}^\dagger\boldsymbol{\tau}\Xi + \bar{\Xi}\gamma^\mu\gamma_5\boldsymbol{\tau}\partial_\mu\bar{K}\cdot\boldsymbol{\Sigma}\right] - f_{NN\eta_8}\bar{N}\gamma^\mu\gamma_5 N\partial_\mu\eta\\ &-f_{\Lambda\Lambda\eta_8}\bar{\Lambda}\gamma^\mu\gamma_5\Lambda\partial_\mu\eta - f_{\Sigma\Sigma\eta_8}\overline{\boldsymbol{\Sigma}\cdot}\gamma^\mu\gamma_5\boldsymbol{\Sigma}\partial_\mu\eta - f_{\Xi\Xi\eta_8}\bar{\Xi}\gamma^\mu\gamma_5\Xi\partial_\mu\eta\end{aligned}$$

SU$_f$(3) relations

$$g_A = F + D \cong 1.26,\ \ \alpha = F/(F+D),\ \ f_{NN\pi} = f = \frac{g_A}{2F_\pi},\ \ f_{\Xi\Xi\pi} = -(1-2\alpha)f,$$

$$f_{\Lambda NK} = -\frac{1}{\sqrt{3}}(1+2\alpha)f,\ f_{\Lambda\Sigma\pi} = \frac{2}{\sqrt{3}}(1-\alpha)f,\ f_{\Sigma\Sigma\pi} = 2\alpha f,\ f_{\Sigma NK} = (1-2\alpha)f,\ \cdots$$

Strangeness $S=-1$: Leading-Order in ChEFT

- H. Polinder, J. Haidenbauer, and U.-G. Meißner, Nucl. Phys. A779, 244 (2006)
- Contact terms without derivative, and one pseudoscalar-meson (π, K, η) exchange
- Leading-order SU$_f$(3) invariants $\mathcal{L}_{BBBB} = c_i(\bar{B}\Gamma_i B)(\bar{B}\Gamma_i B) + \cdots$

  $[\ \Gamma_1 = 1,\ \Gamma_2 = \gamma^\mu,\ \Gamma_3 = \sigma^{\mu\nu},\ \Gamma_4 = \gamma^\mu\gamma_5,\ \Gamma_5 = \gamma_5\ ]$

  Non-relativistic reduction gives

$$\mathcal{L}_{BBBB} = \sum_{ijkl=1}^{3}\{c_{00}^{1}(B_{ij}B_{jk})(B_{kl}B_{li}) + c_{00}^{2}(B_{ij}\boldsymbol{\sigma}B_{jk})\cdot(B_{kl}\boldsymbol{\sigma}B_{li}) + c_{00}^{3}(B_{ij}B_{kl})(B_{jk}B_{li})$$
$$+c_{00}^{4}(B_{ij}\boldsymbol{\sigma}B_{kl})\cdot(B_{jk}\boldsymbol{\sigma}B_{li}) + c_{00}^{5}(B_{ij}B_{ji})(B_{kl}B_{lk}) + c_{00}^{6}(B_{ij}\boldsymbol{\sigma}B_{ji})\cdot(B_{kl}\boldsymbol{\sigma}B_{lk})\}$$

- In YN ($S=-1$) at LO, there are 5 S-wave contact low-energy constants
  - （c_{00}^{i} are reorganized） $C_{1S0}^{\Lambda N-\Lambda N}, C_{3S1}^{\Lambda N-\Lambda N}, C_{1S0}^{\Sigma N-\Sigma N}, C_{3S1}^{\Sigma N-\Sigma N}, C_{3S1}^{\Lambda N-\Sigma N}$
- One ps-meson exchange potential is familiar (OBEP)

$$V_{B_1B_2\to B_3B_4} = -f_{B_1B_3P}f_{B_2B_4P}\frac{(\boldsymbol{\sigma}_1\cdot\boldsymbol{q})(\boldsymbol{\sigma}_2\cdot\boldsymbol{q})}{\boldsymbol{q}^2+m_P^2}\times\text{[isospin factor]}$$

  - SU3 relations are used for coupling constants $f_{B_1B_3P}$.

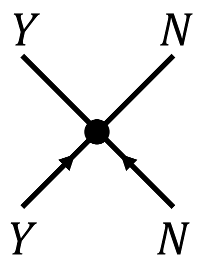

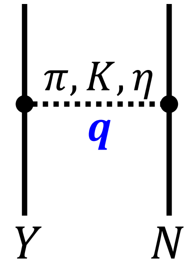

Strangeness $S = -1$: Next-to-Leading-Order in ChEFT

- Haidenbauer, Petschauer, Kaiser, Meißner, Nogga, and Weise, Nucl. Phys. A915, 24 (2013).

- Contact terms with one derivative, and two-ps-meson exchange
- NLO contact terms （low-energy constants: 8 in s-wave and 10 in p-waves）

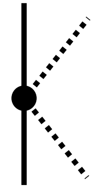

$$V^{(2)}_{BB\to BB} = C_1\boldsymbol{q}^2 + C_2\boldsymbol{k}^2 + (C_3\boldsymbol{q}^2 + C_4\boldsymbol{k}^2)(\boldsymbol{\sigma}_1\cdot\boldsymbol{\sigma}_2) + \frac{i}{2}C_5(\boldsymbol{\sigma}_1+\boldsymbol{\sigma}_2)\cdot(\boldsymbol{q}\times\boldsymbol{k})$$
$$+C_6(\boldsymbol{\sigma}_1\cdot\boldsymbol{q})(\boldsymbol{\sigma}_2\cdot\boldsymbol{q}) + C_7(\boldsymbol{\sigma}_1\cdot\boldsymbol{k})(\boldsymbol{\sigma}_2\cdot\boldsymbol{k}) + \frac{i}{2}C_8(\boldsymbol{\sigma}_1-\boldsymbol{\sigma}_2)\cdot(\boldsymbol{q}\times\boldsymbol{k})$$

- Leading-order $SU_f(3)$ invariant MMBB coupling Lagrangian $\mathcal{L}_2 = \frac{1}{4f_0^2}tr\left(i\bar{B}\gamma^\mu\left[\left[P,\partial_\mu P\right],B\right]\right)$

- Experimental data is insufficient to go to higher orders (NNLO, N^3LO, …)

NLO diagrams

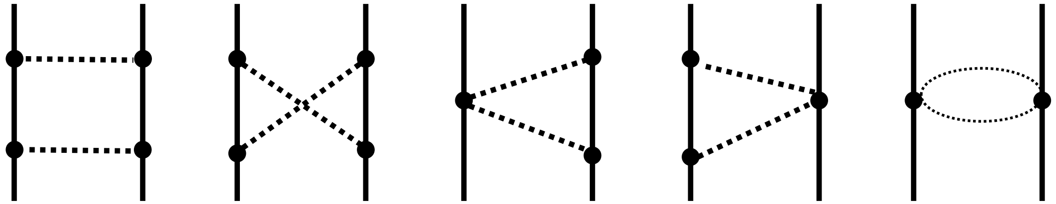

NNLO diagrams

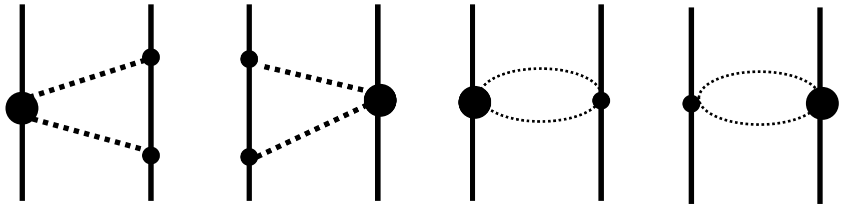

Haidenbauer, Meißner, Nogga, and Le, EPJA (2023) 59-63

3-baryon interactions in SU(3) chiral effective field theory

- Petschauer, Kaiser, Haidenbauer, Meißner, Weise, P. R. C93, 014001 (2016)

- Leading 3-baryon diagrams

diagrams with the power $\nu = 2 + 2L + \sum_i (d_i + \frac{n_i}{2} - 2) = 3$

(d_i and n_i are the number of derivatives and baryon fields, respectively, at the vertex i, and L is the number of loops.)

- Exchanged-meson ϕ is $\pi, K, \mathrm{or}\ \eta$, depending on the baryon B.

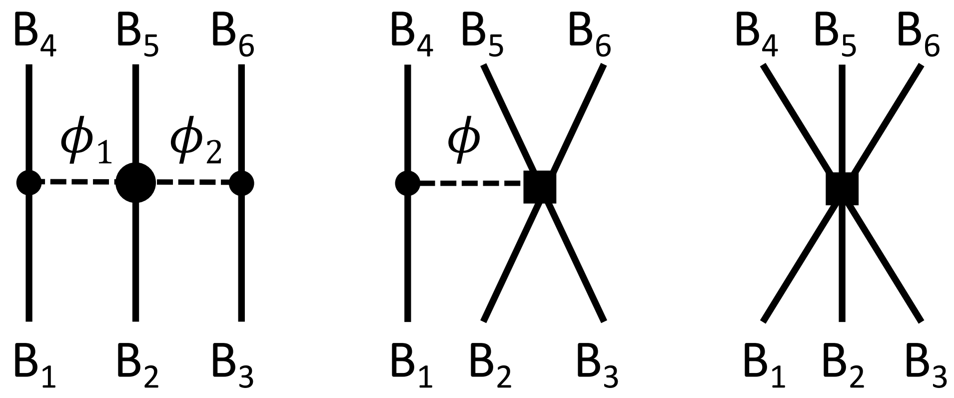

- Various combinations for exchanged mesons are possible, therefore, calculations are complicated.

ΛNN 3-baryon interaction with pion exchange

- ΛNN interaction with 2π exchange （no $\pi\Lambda\Lambda$ vertex, but $\pi\pi\Lambda\Lambda$ is present）

$$V_{3N}^{(2\pi)} = \frac{g_A^2}{3f_\pi^4}\frac{(\boldsymbol{\sigma_3}\cdot\boldsymbol{q_3})(\boldsymbol{\sigma_2}\cdot\boldsymbol{q_2})}{(\boldsymbol{q}_3^2+m_\pi^2)(\boldsymbol{q}_3^2+m_\pi^2)}(\tau_2\cdot\tau_3)[-(3b_0+b_D)m_\pi^2+(2b_2+3b_4)\boldsymbol{q_3}\cdot\boldsymbol{q_2}]$$

- It is not possible, at present, to determine NNLO coupling constants by experimental data.
- Petschauer *et al.* [Nucl. Phys. A957, 347 (2017)] estimated coupling constants by the decouplet saturation model.

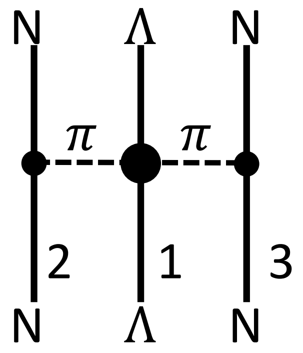

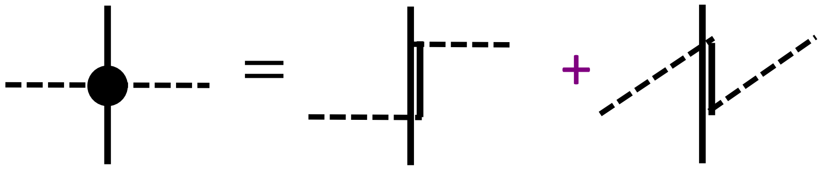

- 1π exchange and contact ΛNN 3-baryon interaction

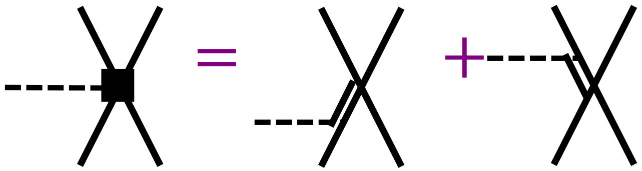

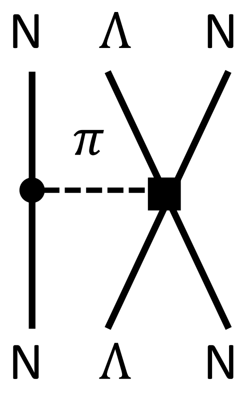

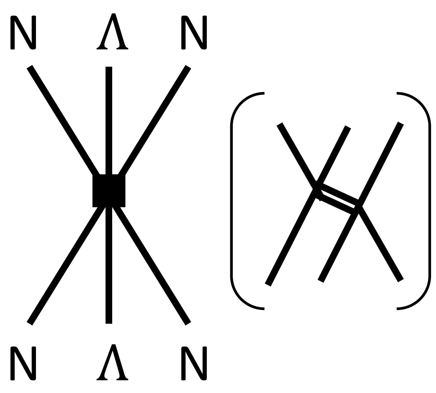

ΛN interactions in the nuclear medium

- Medium effects
  ① Dispersion relation: potential insertion to the propagator
  ② Pauli effects for $\Lambda N - \Lambda N$ correlation and $\Lambda N - \Sigma N$ coupling
    - tensor force is weak in $\Lambda N - \Lambda N$ because of no one-pion exchange, but strong in $\Lambda N - \Sigma N$.
  ③ Three-body forces
- ① and ② are taken care of by G-matrix equation
  - $G(\omega) = v + v\frac{Q}{\omega-(t+U+t+U)}G(\omega)$
  - $U(k) = \sum_{k'}\langle kk'|G(\omega = e_k + e_{k'})|kk'\rangle$
  - $e_k = t(k) + U(k)$
- 3BFs are incorporated by the normal-ordered prescription (density-dependent effective two-body interaction)

$$\langle ab|v_{12(3)}|cd\rangle_A \equiv \frac{1}{2}\sum_h\langle abh|v_{123}|cdh\rangle_A$$

- 1π-exchange and contact terms are excluded.
  (coupling constants are uncertain even in sign.)

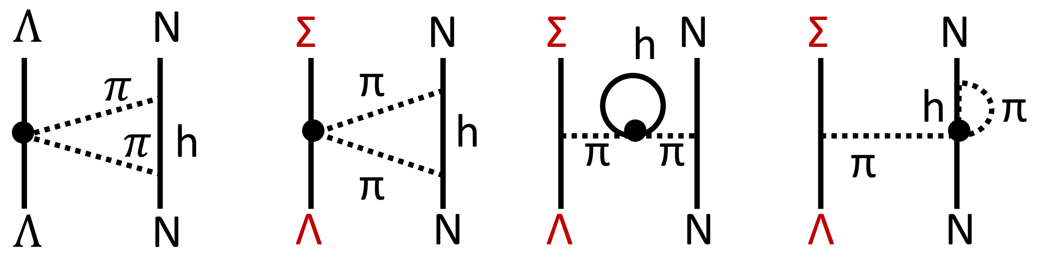

Neutron star matter and hyperons: hyperon puzzle

- Conventional knowledge of attractive Λ-N interactions from the experimental data of hypernuclei ⟹ Λ hyperons appear in high-density neutron star matter to avoid the increase of the neutron chemical potential.
  - Even the standard neutron stars with the mass of $1.4M_{\odot}$ cannot be supported.
- To make the matter worse, heavy neutron stars were observed.
  - PSR J1903+0327 ($1.667 \pm 0.021\ M_{\odot}$), PSR J1614-2230 ($1.928 \pm 0.017\ M_{\odot}$), PSR J0348+0432 ($2.01 \pm 0.04\ M_{\odot}$), PSR J0740+6620 ($2.14^{+0.10}_{-0.09}\ M_{\odot}$)
  - Observation of binary NS merger GW170817 suggests that maximum mass is $2.3 - 2.4\ M_{\odot}$
- To understand heavy neutron stars, the EoS of neutron star matter has to be hard.
  - Appearance of hyperons in neutron star matter is unfavorable: hyperon puzzle
  - Appearance of Δ isobars is unfavorable: Δ puzzle

Neutron stars

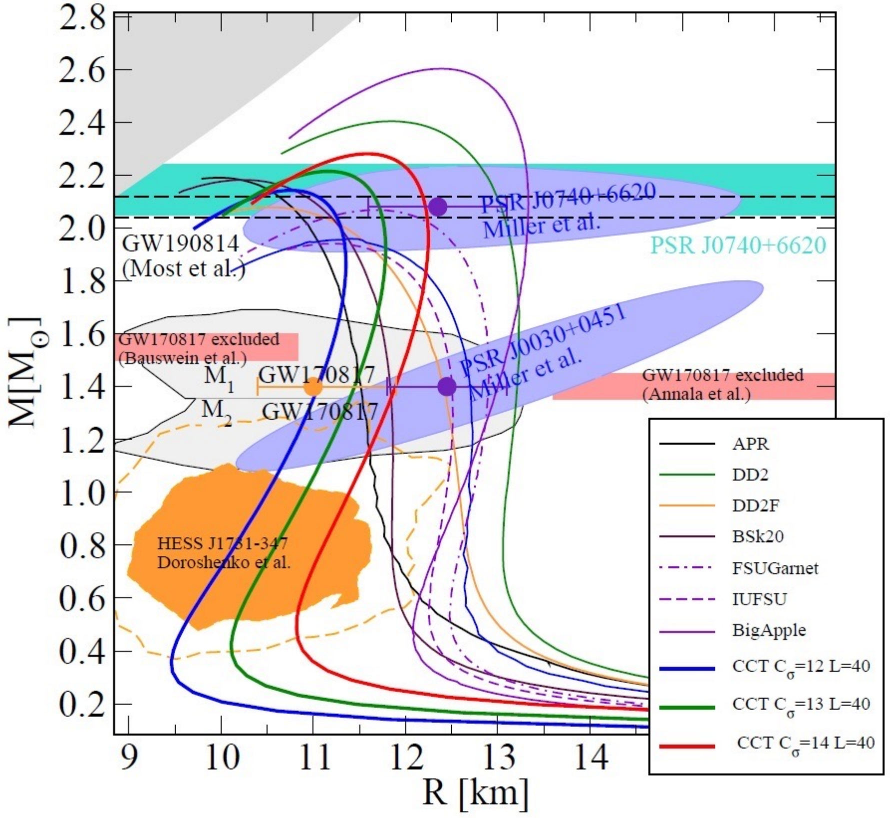

Kubis et al., arXiv:2307.02979V1, Fig.1

- NS with a small mass and a compact size

  $M = 0.77^{+0.20}_{-0.17} M_{\odot}$,

  $R = 10.4^{+0.86}_{-0.78}$ km

- Doroshenko et al., Nature Astron. 6, 1444 (2022)]

Heuristic 2nd order calculations

- Pauli blocking effect for the Σ^* excitation in the nuclear medium (pure neutron matter)

  (Attractive contribution of the Σ^* excitation in free space is suppressed in the nuclear medium)

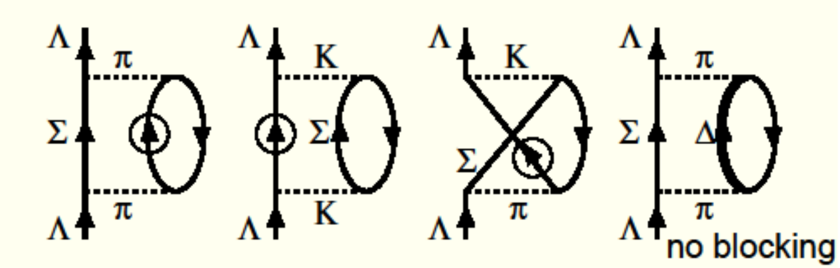

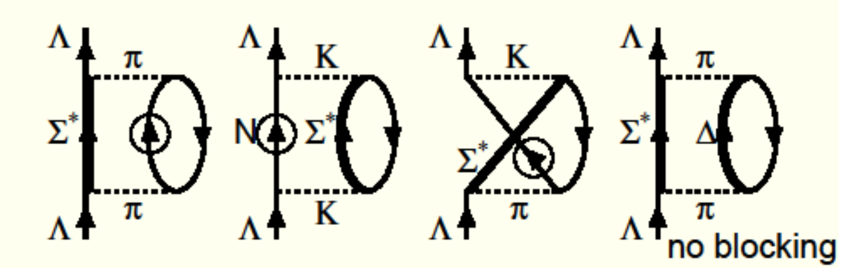

- coupling constants used (vertex form factor $e^{-(q/\Lambda)^2}$ with $\Lambda = 0.96$ GeV)

  $g_{\pi NN} = 12.677,\ g_{\pi\Lambda\Sigma} = 12.677,\ g_{KN\Lambda} = -11.448,\ g_{KN\Sigma} = 0.7032,\ f_{KN\Sigma^*} = -3.22,\ f_{\pi\Lambda\Sigma^*} = 1.106$

blocking of Σ excitation (MeV)			
$\rho_0/2$	ρ_0	$3\rho_0/2$	$2\rho_0$
+0.52	+1.83	+3.58	+5.53

included in G-matrix calculations

blocking of Σ^* excitation (MeV)			
$\rho_0/2$	ρ_0	$3\rho_0/2$	$2\rho_0$
+0.80	+3.79	+9.48	+18.11

not included in G-matrix calculations

➢ Single-particle potentials are included for N, Λ, and Σ propagators

Heuristic 2nd order calculations

- Repulsive contribution of three-body forces with the Σ^* intermediate excitation is expected to be large, in addition to the Pauli blocking effect for the $\Lambda\mathrm{N} - \Sigma N$ coupling.

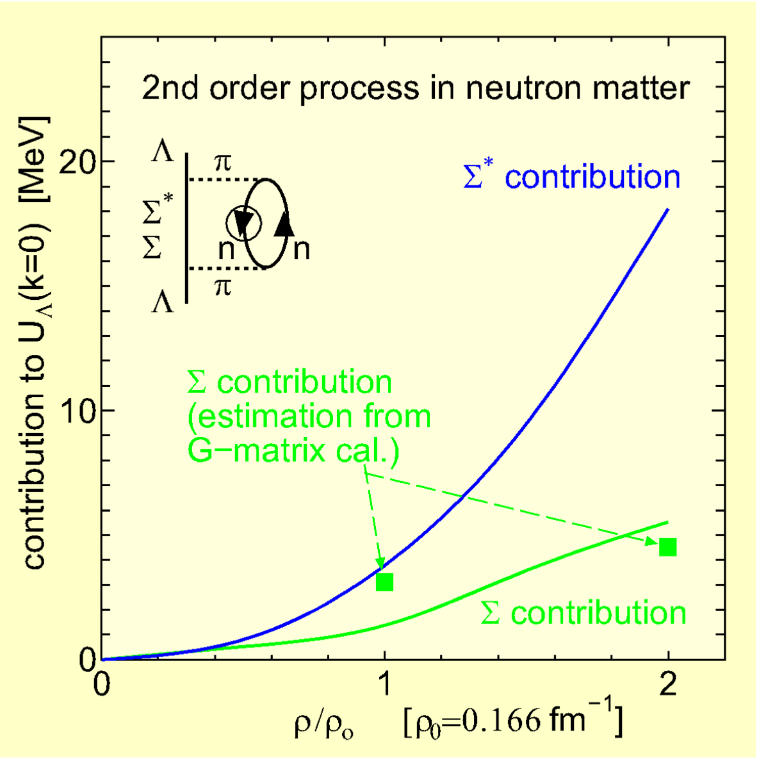

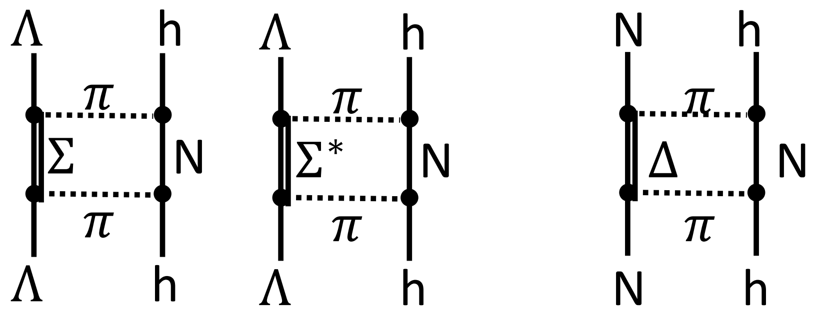

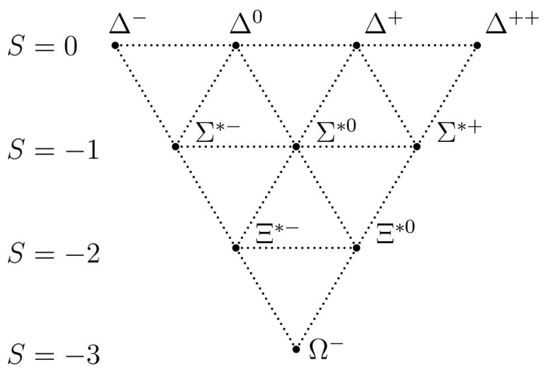

Density dependence of $U_\Lambda(0)$ in symmetric nuclear matter (NLO13)

- LOBT calculations in symmetric nuclear matter (SNM)
- 3BF contributions are attractive in the $^3S_1$-state (as in the case of 3NFs) and repulsive in P-states
  - $U_\Lambda(0) \sim -30$ MeV is reasonable, compared with the empirical single-particle potential depth.

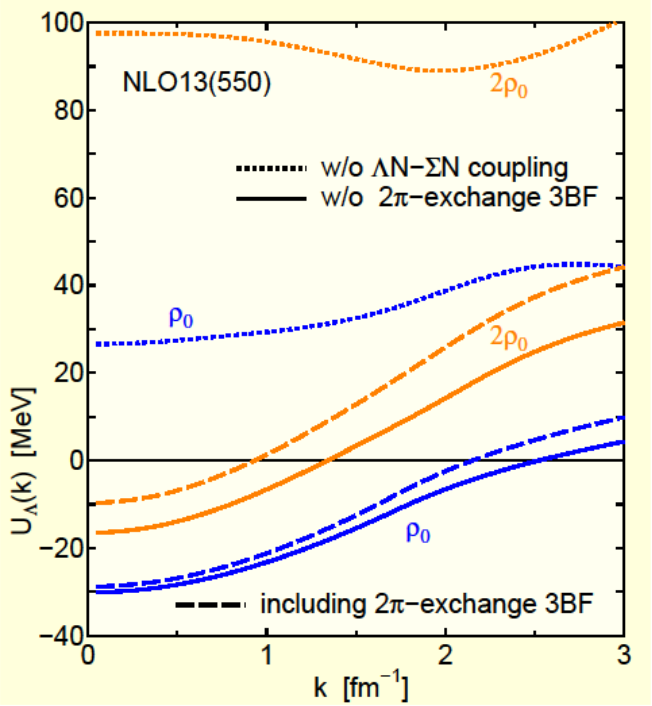

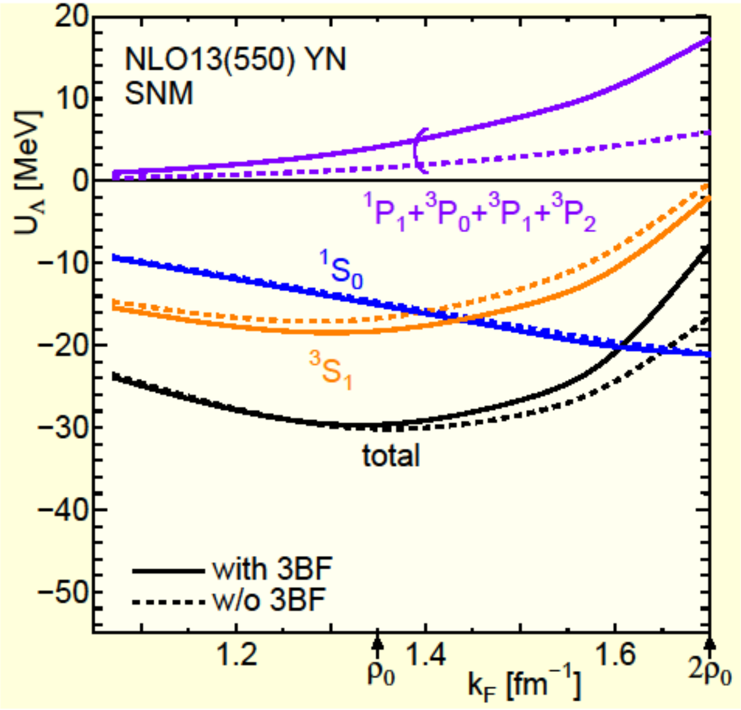

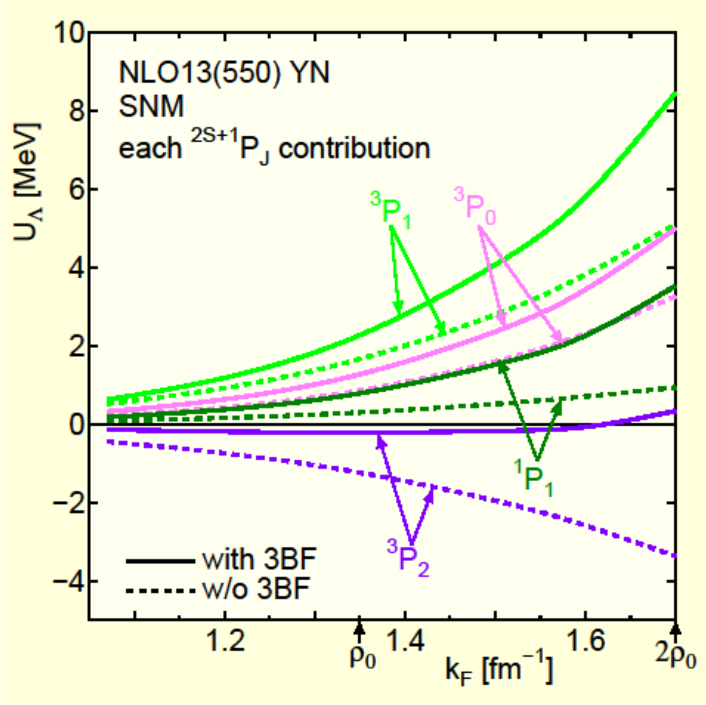

Density dependence of $U_\Lambda(0)$ in symmetric nuclear matter (NLO19)

- No difference in P waves between NLO13 and NLO19
- The $^3S_1$ attraction of NLO19 is larger than that of NLO13, despite the weaker the $\Lambda N - \Sigma N$ coupling
  - Note that the 3BF parameters are same for NLO13 and NLO19

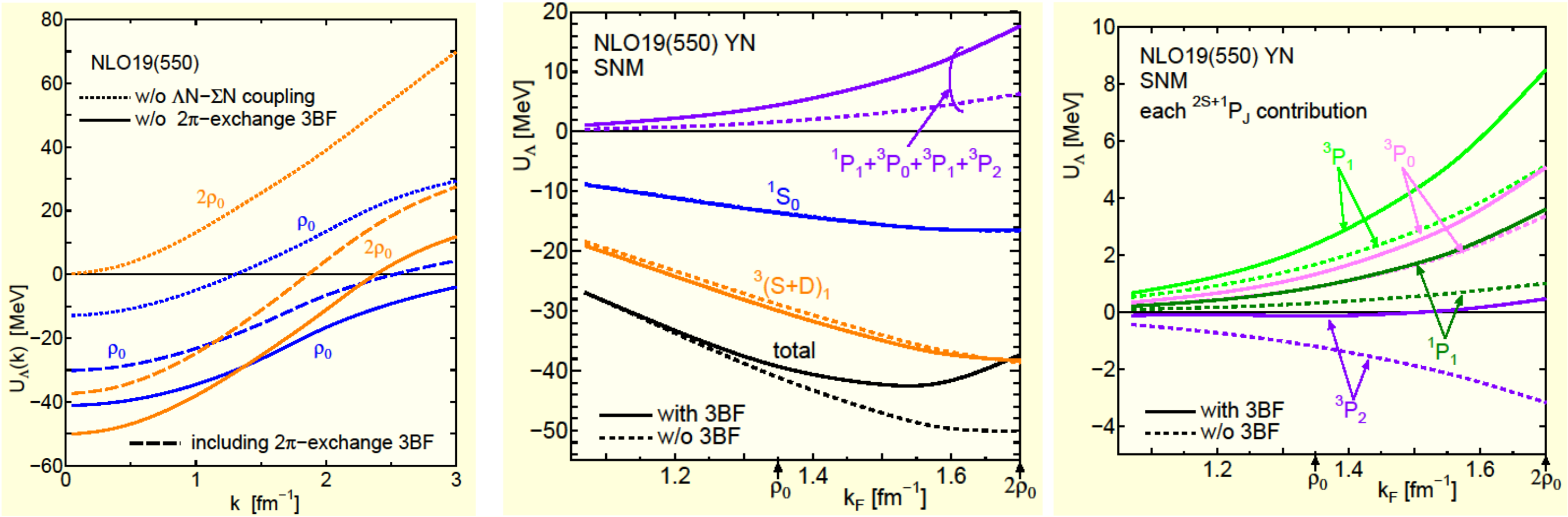

Role of ΛN-ΣN coupling (ChEFT interactions)

- Calculations by switching off the ΛN-ΣN coupling
  - The coupling strength is model-dependent (not observable)
  - The coupling is stronger in NLO13 than in NLO19.

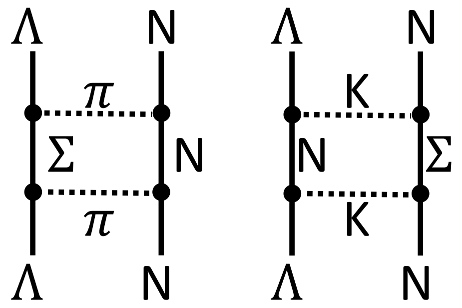

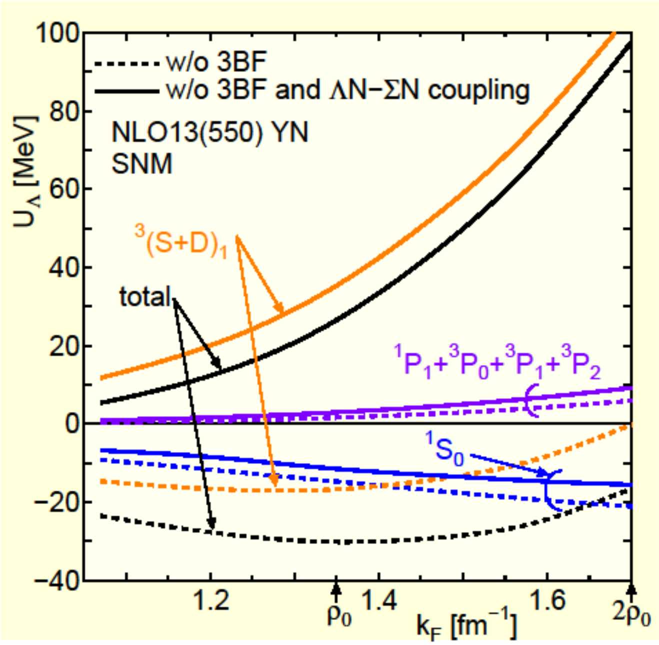

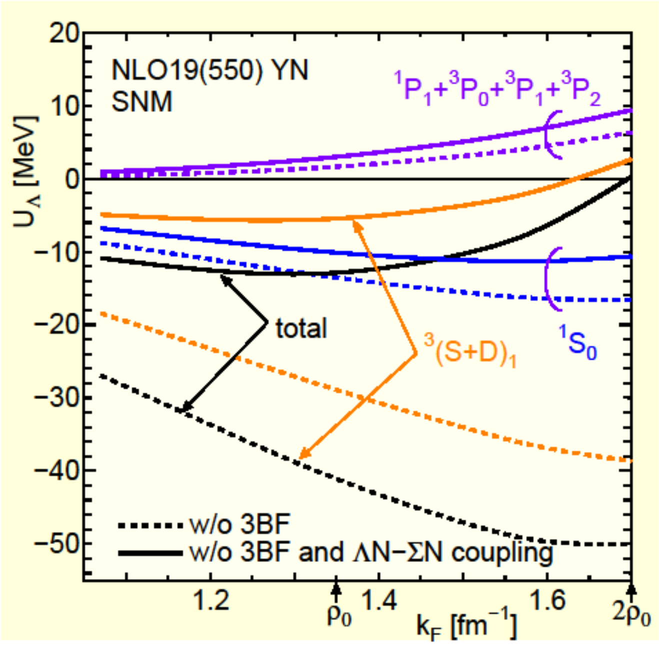

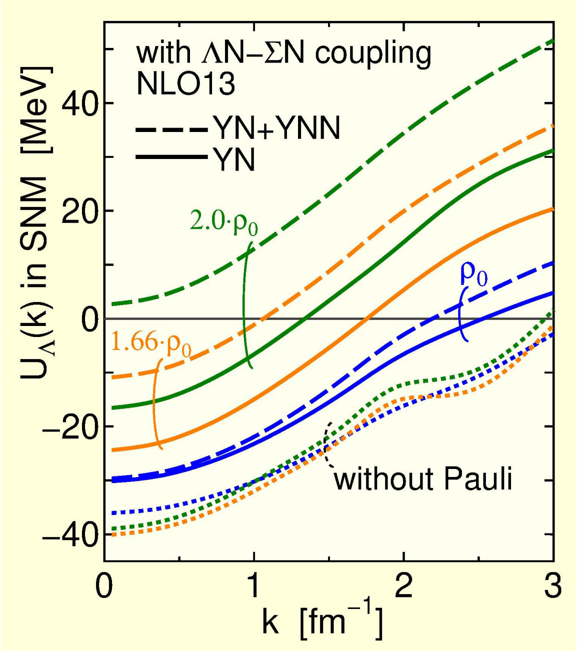

Role of ΛN-ΣN coupling

- Calculations by switching off the ΛN-ΣN coupling
  - The coupling strength is model-dependent (not observable)
  - The coupling is strong in NLO13 and NSC97, relatively weak in fss2 (and NLO1).
  - In the nuclear medium, ΛN-ΣN coupling is partly Pauli blocked.

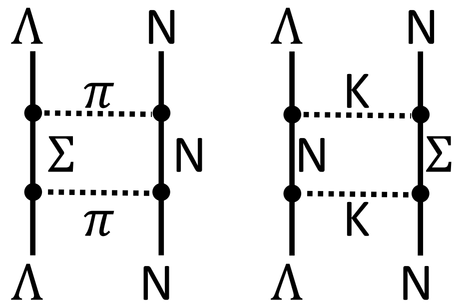

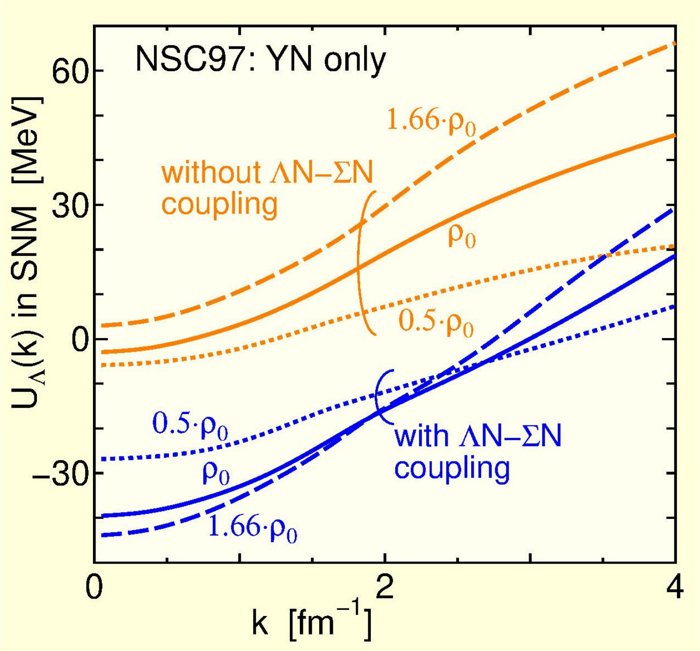

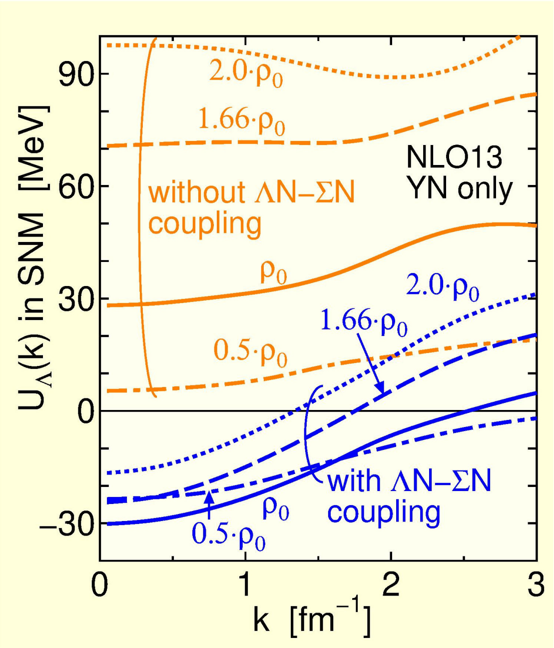

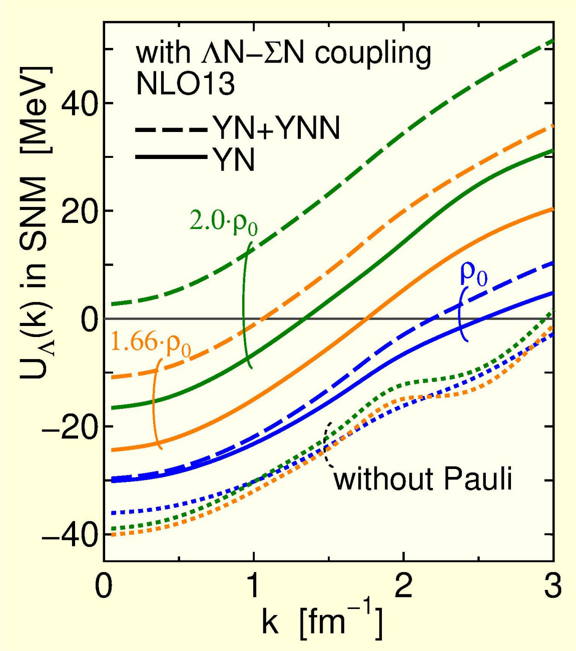

Λ chemical potential in neutron star matter

- M. Kohno, Phys. Rev. C97, 035206 (2018) calculations with NLO13 YN interactions

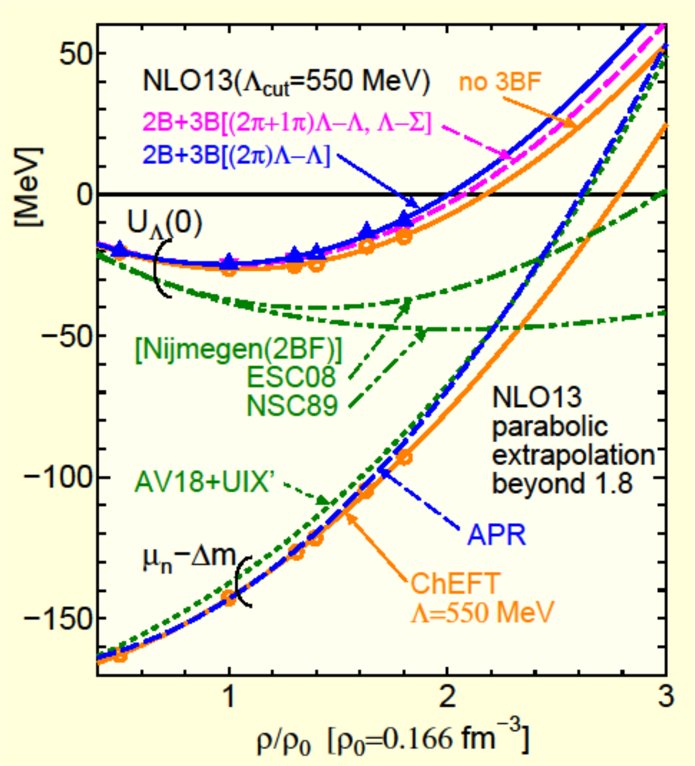

- Calculations by the München group: "Hyperon-nucleon three-body forces and strangeness in neutron stars", Gerstung, Kaiser, and Weise, E.P.J. 56, 175 (2020). NLO13 YN interactions

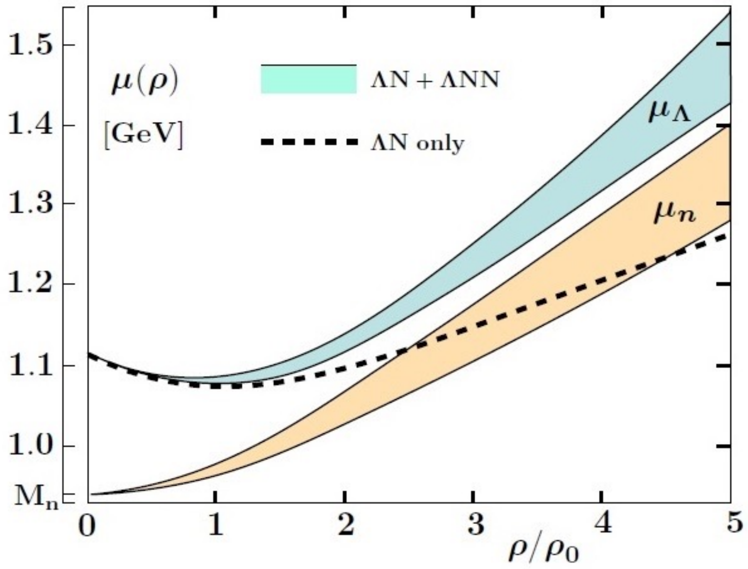

➢ Critical point depends on μ_N.

- G-matrix calculations in pure neutron matter involving density-dependent two-body interactions normal-ordered from ΛNN and ΛNN-ΣNN 3BFs (2π exchange).
  - Hyperon puzzle is resolved?
  - Large uncertainties even in the sign of the coupling constants.
  - The results would change when either NLO19 or NNLO is employed.

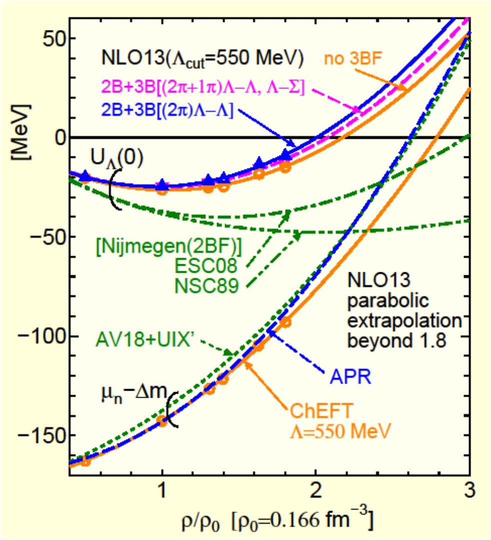

- Necessary to improve YN and YNN interactions
  - Experimental data
    - Hypertriton, direct YN scattering, and momentum correlation function
  - Theoretical studies
    - Higher orders and parameters in ChEFT and/or Lattice data
    - Precise (ab initio) calculations of (light) hypernuclei

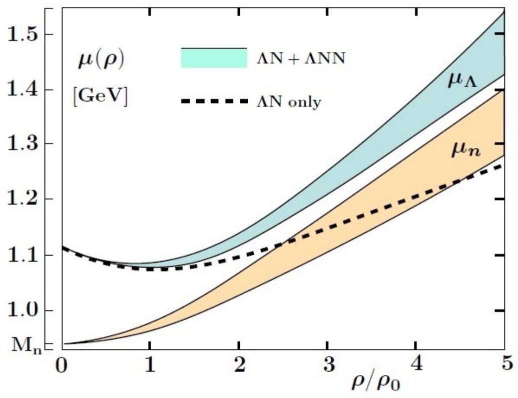

Scenarios that could solve the hyperon puzzle

- Repulsive YN and YY interactions (e.g., by ϕ meson exchange)
  - Difficult to explain hyper nuclei.
- Repulsive effects of 3 baryon forces (YNN, YYN, YYY)
  - It is easy to introduce phenomenological 3BFs, but not so different from the use of the ad hoc EoS ρ^{α}.
  - It is preferable to start with bare YN and YNN interactions.
- Phase transition to quark matter （hybrid star）
  - It is sufficient if the appearance of hyperons is suppressed before the phase change occurs.
  - EoS of the quark matter depends on the model.
- Δ-isobar and/or Kaon condensation？ They, in general, make the matter soft.
  - Δ puzzle
- Presence of dark matter ?
  - Studies based on knowledge of terrestrial hypernuclear data are important.

No-core shell model calculations of light hypernuclei (Jülich group)

- "Benchmarking three-body forces and first predictions for A=3-5 hypernuclei"
  Le, Haidenbauer, Kamda, Kohno, Meißner, Miyagawa, and Nogga, Eur. Phys. J. A. (2025) 61:21
- "Light Hypernuclei Studied with Chiral Hyperon-Nucleon and Hyperon-Nucleon-Nucleon Forces"
  Le, Haidenbauer, Meißner, and Nogga, Phys. Rev. Lett. 134, 072502 (2025)

➢ 3BF parameters: decouplet-saturation model + small adjustment

➢ N^{2}LO YN

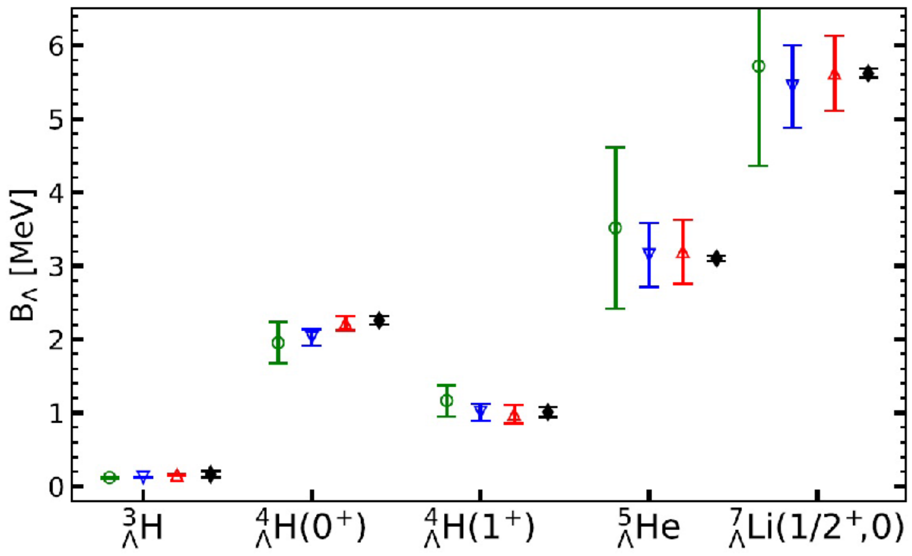

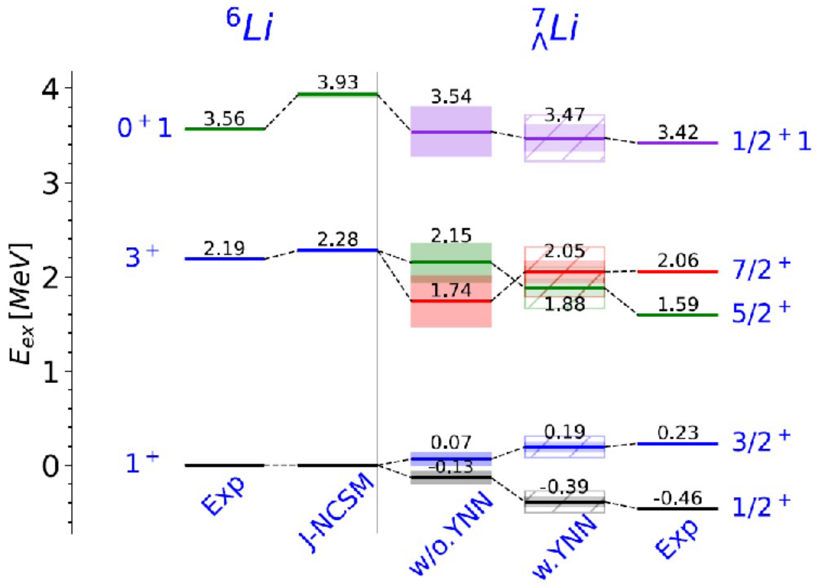

Λ-deuteron correlation function calculated in Faddeev formulation

- The energy of the hypertriton, the lightest bound state, has not been pinned down yet.

  the current world average of the binding energy of ${}^{3}_{\Lambda}\mathrm{H}$ is 164 ± 43 keV

  [P. Eckert *et al.*, Chart of hypernucleids Hypernuclear Structure and Decay Data, 2023, https://hypernuclei.kph.uni-mainz.de.]

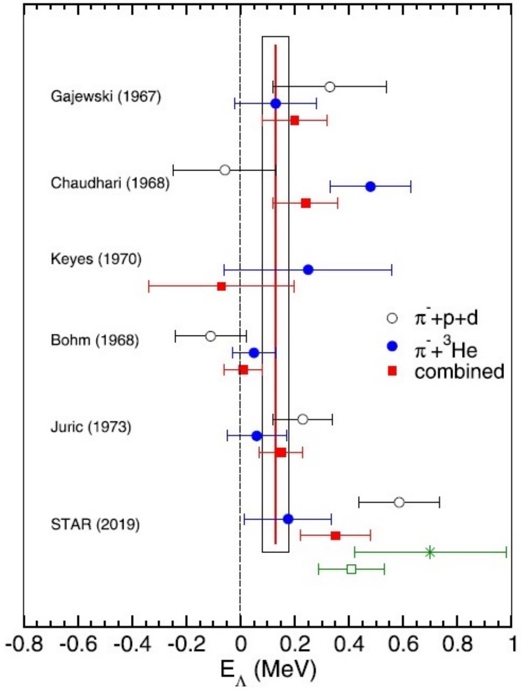

- The spin of the hypertriton is $J = 1/2$.
- The energy calculation does not determine the ration of ${}^{3}V_{\Lambda N}/{}^{1}V_{\Lambda N}$.

- The spin $J = 3/2$ state participate in the scattering process.
- Experiments of the Λ-deuteron scattering are not expected at present.
- The recent advancements of the measurement of the Λd correlation functions provide an alternative source of the information.
- The Λ-deuteron three-body system is calculated in Faddeev formulation.

Two-body ΛN scattering phase shifts: $^1S_0$ and $^3S_1$ channels

- The difference between NLO13 and NLO19
  - NLO13: J. Haidenbauer, S. Petschauer, N. Kaiser, U.-G. Meißner, A. Nogga, W. Weise, Nucl. Phys. A 915, 24 (2013).
  - NLO19: J. Haidenbauer, U.-G. Meißner, and A. Nogga, Eur. Phys. J. A 56, 91 (2020).

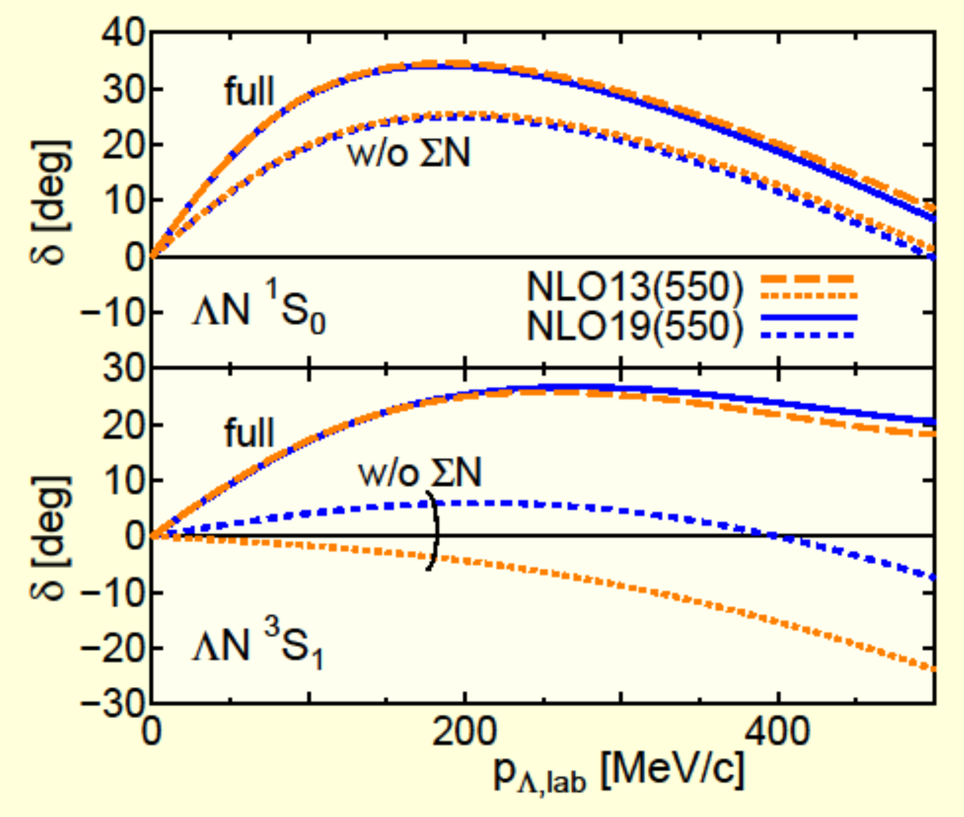

- NLO13 and NLO19 provide same phase shifts both in $^1S_0$ and $^3S_1$ despite of the difference in their ΛN-ΣN coupling strength.
  - Switching off the ΛN-ΣN coupling, the $^3S_1$ ΛN interaction becomes repulsive in NLO13.

Low-energy Λ-deuteron scattering phase shifts: $J = 1/2$ and $J = 3/2$

- $J = 1/2$
  - Because of the constraint that ${}^3_\Lambda\mathrm{H}$ is bound, NLO13 and NLO19 predict same phase shifts.
- $J = 3/2$
  - ${}^3S_1$ of NLO19 is more attractive than that of NLO13
  - The behavior at $E_{cm} \approx 0$ suggests a pole (virtual state) close to the real axis.

    NLO13: $k = -0.08i$ fm^{-1} ($E = -0.17$ MeV)

    NLO19: $k =- -0.05i$ fm^{-1} ($E = -0.07$ MeV)
- Due to the total isospin T=0, ${}^1S_0$ *np* does not participates, therefore δ_I is small.

- NN interactions: chiral N^{4}LO$^+$(550)

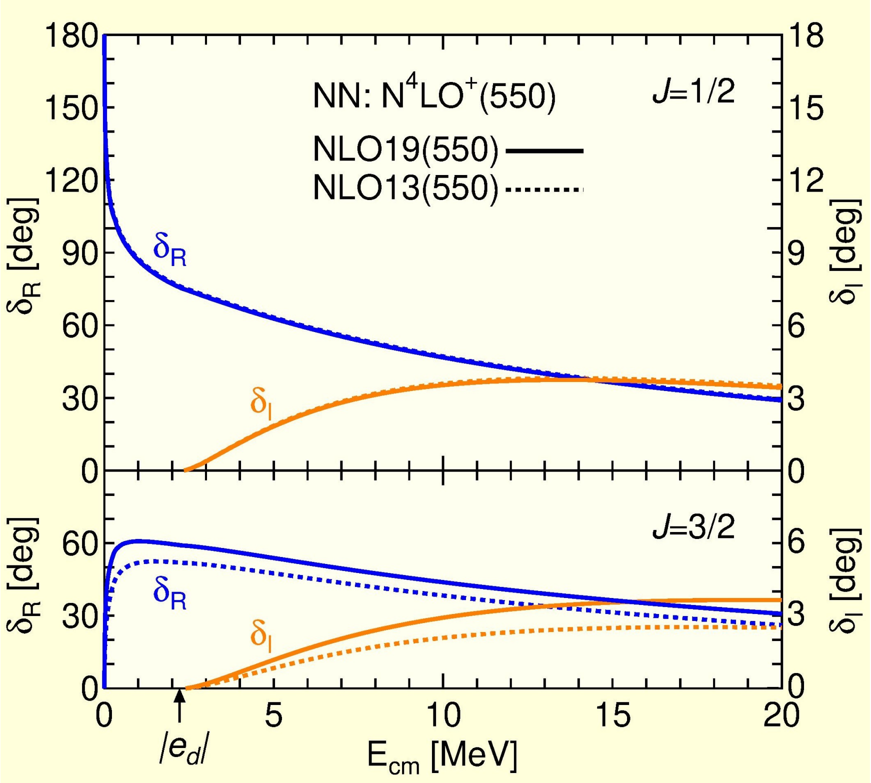

Λ-deuteron correlation function with elastic wave function

$$C^J_{\Lambda d}(k) = 1 + 4\pi \int_0^\infty r^2\, dr S_{12}(r) \left\{ \left|\psi_J(k;r)\right|^2 - |j_0(kr)|^2 \right\}$$

source function with range R: $S_{12}(r) = \frac{1}{(2\sqrt{\pi}R)^3} \exp\left(-\frac{1}{4R^2} r^2\right)$

wave function in r-space from the calculated T-matrix

$$\psi_\ell(k;r) = j_0(kr) + \frac{2\mu_{\Lambda d}}{\hbar^2} \int_0^\infty k'^2\, dk' \frac{j_\ell(k'r) T_{2,\ell}(k',k)}{k^2 + i\eta - k'^2}$$

- Lednicky-Lyuboshits formula [Sov. J. Nucl. Phys. 35, 770 (1982)]

$$C^J_{\Lambda d}(k) \approx 1 + \frac{\left|f_J(k)\right|^2}{2R} F(r_0) + \frac{2\mathrm{Re} f_J(k)}{\sqrt{\pi}R} F_1(x) - \frac{\mathrm{Im} f_J(k)}{R} F_2(x)$$

$$F(r_0) = 1 - \frac{r_e}{2\sqrt{\pi}R}, F_1(x) = \frac{\int_0^x dt\, e^{t^2 - x^2}}{x}, F_2(x) = (1 - e^{-x^2})/x$$

scattering amplitude $f_j \approx \frac{1}{-\frac{1}{a_s} + \frac{1}{2} r_e k^2 - ik}$

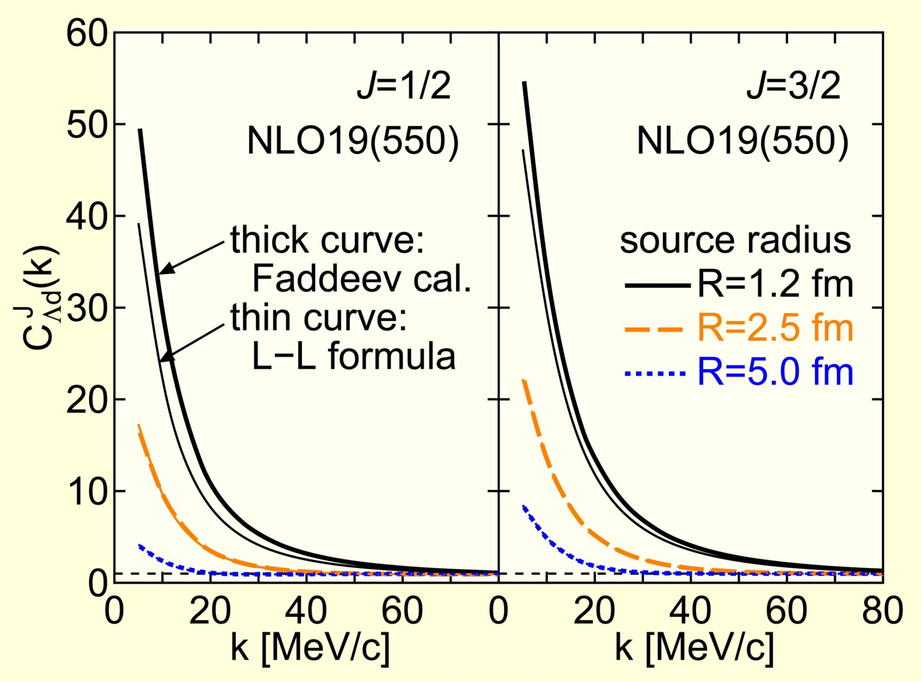

- Results of Faddeev cal. and L-L formula are undistinguishable for $R = 1.2$ fm, 1.5 fm .

Λ-deuteron spin-averaged correlation function

- First experimental (preliminary) data [Yu Hu *et al.*, arXiv:2401.00319v1]

"Measurements of $p\Lambda$ and $d\Lambda$ correlations in 3 GeV Au+Au collisions at STAR"

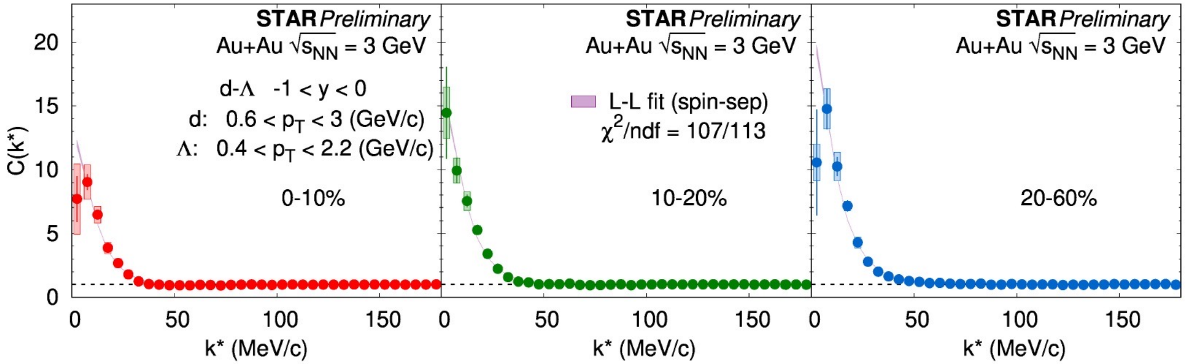

- $J = \frac{1}{2}$

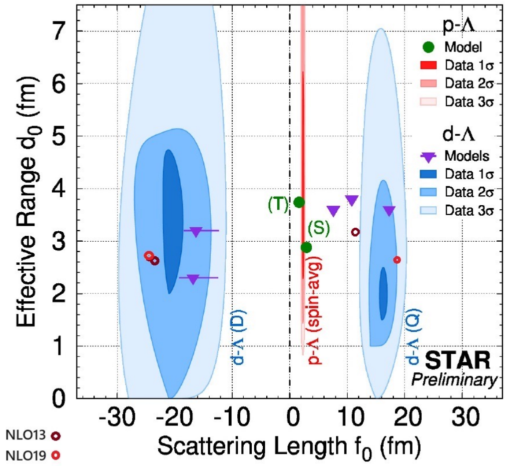

$J = \frac{3}{2}$

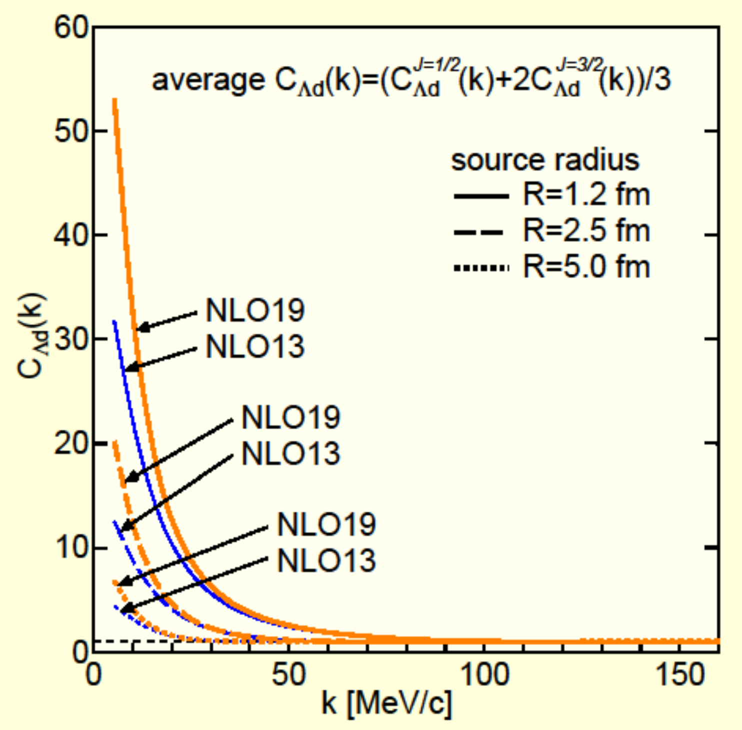

- spin averaged correlation function

Faddeev calculations
with NLO13 and NLO19

Correlation function $R(q)$ (S. Mrówozyńsky [Eur. Phys. J. Spec. Top. 229, 3559(2020)])

$$R(q) = \iiint d\boldsymbol{r}_\Lambda d\boldsymbol{r}_n d\boldsymbol{r}_p\, D(r_\Lambda)D(r_n)D(r_p)|\psi_{\Lambda np}(\boldsymbol{r}_{\Lambda(np)}, \boldsymbol{r}_{np})|^2 \Big/ \iint d\boldsymbol{r}_n d\boldsymbol{r}_p\, D(r_n)D(r_p)|\varphi_d(\boldsymbol{r}_{np})|^2$$

$$\psi_{\Lambda np}(\boldsymbol{r}_{\Lambda(np)}, \boldsymbol{r}_{np}) \xrightarrow[|\boldsymbol{r}_{\Lambda(np)}|, |\boldsymbol{r}_{np}| \to \infty]{} e^{i\boldsymbol{q}_0 \cdot \boldsymbol{r}_{\Lambda(np)}} \psi_d(\boldsymbol{r}_{np})$$

- source function $D(r) = D(r; R_s) \equiv (\sqrt{2\pi}R_s)^{-3} e^{-r^2/(2R_S^2)}$, $D(r)$

$$R(q) = \iint d\boldsymbol{r}_{\Lambda(np)} d\boldsymbol{r}_{np}\, D(r_{\Lambda(np)}; \sqrt{3/2}R_s) D(r_n; \sqrt{2}R_s)|\psi_{\Lambda np}(\boldsymbol{r}_{\Lambda(np)}, \boldsymbol{r}_{np})|^2 / \int d\boldsymbol{r}_{np}\, D(r_{np}; \sqrt{2}R_s)|\varphi_d(\boldsymbol{r}_{np})|^2$$

- Supposing the deuteron is an elementary particle $\psi_{\Lambda np}(\boldsymbol{r}_{\Lambda(np)}, \boldsymbol{r}_{np}) = \psi_{\Lambda d}(\boldsymbol{r}_{\Lambda \mathrm{d}})\varphi_d(\boldsymbol{r}_{np})$,

$$R(q) = \int d\boldsymbol{r}_{\Lambda d}\, D(r_{\Lambda d}; \sqrt{3/2}R_s)\, |\psi_{\Lambda d}(\boldsymbol{r}_{\Lambda \mathrm{d}})|^2$$ (note that the range is $\sqrt{3/2}R_s$ instead of $\sqrt{2}R_s$)

- Assume that the Λdrelative wave function differs from the plane $e^{i\boldsymbol{q}_0 \cdot \boldsymbol{r}_{\Lambda d}}$ only in the s wave,

$$\psi_{\Lambda np}(\boldsymbol{r}_{\Lambda(np)}) = e^{i\boldsymbol{q}_0 \cdot \boldsymbol{r}_{\Lambda d}} - j_0(r_{\Lambda d}) + \psi_{\Lambda d}^{l=0}(r_{\Lambda \mathrm{d}})$$

$$R(q) \cong 1 + 4\pi \int r_{\Lambda d}^2 dr_{\Lambda d}\, D(r_{\Lambda d}; \sqrt{3/2}R_s) \{|\psi_{\Lambda d}^{l=0}(r_{\Lambda \mathrm{d}})|^2 - |j_0(r_{\Lambda d})|^2\}$$

➢ When $\psi_{\Lambda d}^{l=0}(r_{\Lambda \mathrm{d}})$ is described by effective range parameters, L-L formula is obtained.

Correlation function $R(q)$ (S. Mrówozyńsky [Eur. Phys. J. Spec. Top. 229, 3559(2020)])

- In the case of $\psi_{\Lambda np}(\boldsymbol{r}_{\Lambda(np)}, \boldsymbol{r}_{np}) \neq \psi_{\Lambda d}(\boldsymbol{r}_{\Lambda \mathrm{d}})\varphi_d(\boldsymbol{r}_{np})$

$$R(q) = \iint d\boldsymbol{r}_{\Lambda(np)} d\boldsymbol{r}_{np}\, D\left(r_{\Lambda(np)}; \sqrt{3/2}R_s\right) D\left(r_n; \sqrt{2}R_s\right) |\psi_{\Lambda np}(\boldsymbol{r}_{\Lambda(np)}, \boldsymbol{r}_{np})|^2 / \int d\boldsymbol{r}_{np}\, D\left(r_{np}; \sqrt{2}R_s\right) |\varphi_d(\boldsymbol{r}_{np})|^2$$

source function $D(r) = D(r; R_s) = (\sqrt{2\pi}R_s)^{-3} e^{-r^2/(2R_S^2)}$

- Supposing that only the s-wave is altered from the plane wave $e^{i\boldsymbol{q}_0 \cdot \boldsymbol{r}_{\Lambda d}}$

$$R(q) \times \int d\boldsymbol{r}_{np}\, D\left(r_{np}; \sqrt{2}R_s\right) |\varphi_d(\boldsymbol{r}_{np})|^2$$
$$\cong 1 + (4\pi)^2 \iint r_{\Lambda d}^2 dr_{\Lambda d} r_{np}^2 dr_{np}\, D\left(r_{\Lambda d}; \sqrt{3/2}R_s\right) D\left(r_{np}; \sqrt{2}R_s\right) \left(|\psi_{\Lambda np}\left(r_{\Lambda d}, r_{np}\right)|^2 - |j_0(r_{\Lambda d})|^2 |\varphi_d(\boldsymbol{r}_{np})|^2\right)$$

- The source radius is different between r_{np} and $r_{\Lambda d}$. ($r_{\Lambda d}$ is not $\sqrt{2}R_s$, but $\sqrt{3/2}R_s$)

Three-body wave function in Faddeev formulation

- For incident Λd wave ϕ, full wave function $\Psi^{(+)} = \lim_{\varepsilon\to 0} i\varepsilon \frac{1}{E+i\varepsilon-H}\phi = \Psi_1^{(+)} + \Psi_2^{(+)} + \Psi_3^{(+)}$
  - $H = H_0 + V_{12} + V_{23} + V_{31}$ （H_0 kinetic energy in the CM system)
- Rewriting $(H_0 + V_1 + V_2 + V_3 - E)\Psi^{(+)} = 0$ to $\Psi^{(+)} = G_0(V_1 + V_2 + V_3)\Psi^{(+)}$ $\left[G_0 = \frac{1}{E-H_0}\right]$
- $u_3|\phi\rangle \equiv (V_{31} + V_{23})|\Psi^{(+)}\rangle$ and introducing two-body t-matrix t_3 ($i = 3$ is assigned to Λ)

  Faddeev equation becomes $u_3\phi = (1 - P_{12})t_2G_0u_2\phi$, $u_2\phi = G_0^{-1}\phi + t_3G_0u_3\phi - P_{12}t_2G_0u_2\phi$

  Introducing $T_i \equiv t_iG_0u_i$, then $T_3\phi = t_3G_0(1 - P_{12})T_2\phi$, $T_2\phi = t_2\phi + t_2G_0T_3\phi - t_2P_{12}G_0T_2\phi$
- Inserting complete set of the plane wave $|\phi_0\rangle\langle\phi_0| = 1$, the wave function is written as

$$\begin{aligned}\langle \boldsymbol{r}_{\Lambda(np)}, \boldsymbol{r}_{np}|\Psi^{(+)}\rangle &= \langle \boldsymbol{r}_{\Lambda(np)}, \boldsymbol{r}_{np}|G_0|\phi_0\rangle\langle\phi_0|V_{12} + V_{23} + V_{31}|\Psi^{(+)}\rangle \\ &= \langle \boldsymbol{r}_{\Lambda(np)}, \boldsymbol{r}_{np}|G_0|\phi_0\rangle\langle\phi_0|G_0^{-1} + 2T_2 + T_3|\phi\rangle \\ &= \langle \boldsymbol{r}_{\Lambda(np)}, \boldsymbol{r}_{np}|\phi\rangle + \langle \boldsymbol{r}_{\Lambda(np)}, \boldsymbol{r}_{np}|G_0|\phi_0\rangle\langle\phi_0|2T_2 + T_3|\phi\rangle\end{aligned}$$

Wave function in the incident channel

- Λd incident channel: $\left\langle \boldsymbol{r}_{\Lambda(np)}, \boldsymbol{r}_{np} \middle| \Psi_3^{(+)} \right\rangle = \langle \boldsymbol{r}_{\Lambda(np)}, \boldsymbol{r}_{np} | \phi \rangle + \langle \boldsymbol{r}_{\Lambda(np)}, \boldsymbol{r}_{np} | G_3 | \phi_0 \rangle \langle \phi_0 | 2T_2 | \phi \rangle$
  - channel Green function $G_3 = \frac{1}{E - H_0 - V_{12}}$ $\quad (V_{12} = V_{np})$
  - To explicitly evaluate $\langle \boldsymbol{r}_{\Lambda(np)}, \boldsymbol{r}_{np} | G_3 | \phi_0 \rangle$, the eigen functions $|\Phi\rangle$ of $H_0 + V_3$ are used.

    $\Rightarrow \langle \boldsymbol{r}_{\Lambda(np)}, \boldsymbol{r}_{np} | G_3 | \Phi \rangle \langle \Phi | \phi_0 \rangle$ (note that wave function $\langle \Phi | \phi_0 \rangle$ is a generalized function)
- Spectral representation of the Green function (s-wave) $\quad [\ |\Phi\rangle\langle\Phi| = |\Phi_d\rangle\langle\Phi_d| + |\Phi_{scat}\rangle\langle\Phi_{scat}|\ ]$

$$\langle r_{\Lambda(np)}, r_{np} | G_3 | \Phi_d\ , \Phi_{scat} \rangle * = \int q^2 dq \frac{\varphi_d(r_{np}) j_o(q r_{\Lambda(np)})}{E + |e_d| - \frac{\hbar^2}{2\mu_{\Lambda np}} q^2 + i\mathcal{E}} * , \qquad \frac{2}{\pi} \iint p^2 dp\, q^2 dq \frac{\psi_p(r_{np}) j_o(q r_{\Lambda(np)})}{E - \frac{\hbar^2}{2\mu_{np}} p^2 - \frac{\hbar^2}{2\mu_{\Lambda np}} q^2 + i\mathcal{E}} *$$

  - $\varphi_d(r_{np})$ and $\psi_p(r_{np})$: bound state and scattering state wave functions of $T_3 + V_{12}$
  - Φ_d term corresponds to the elastic and the second term describes breakup in this channel

Contributions of deuteron breakup

- Using three-body wave functions calculated by Faddeev equations

  Incident channel breakup contributions are negligible and rearrangement channel breakup is small.

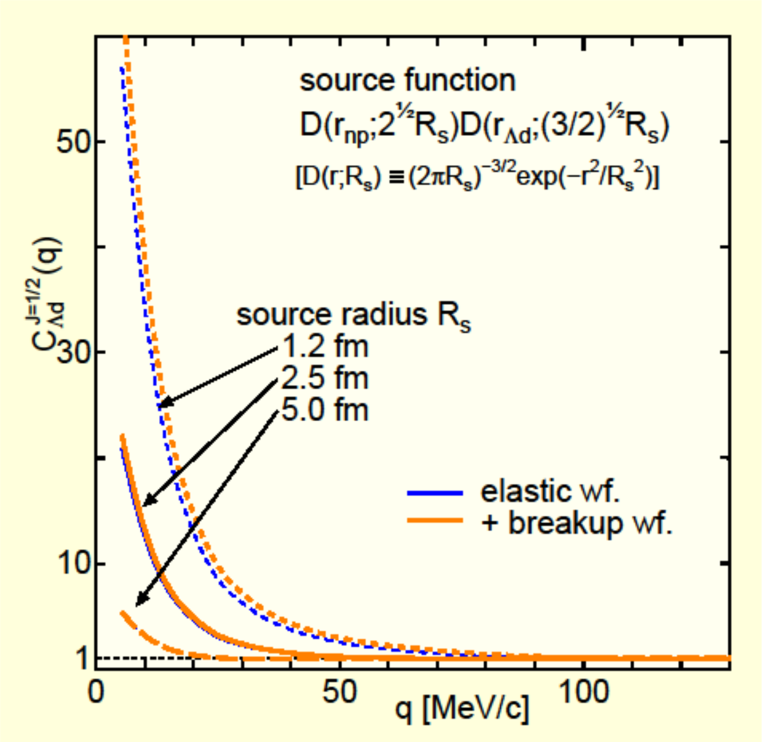

linear scale

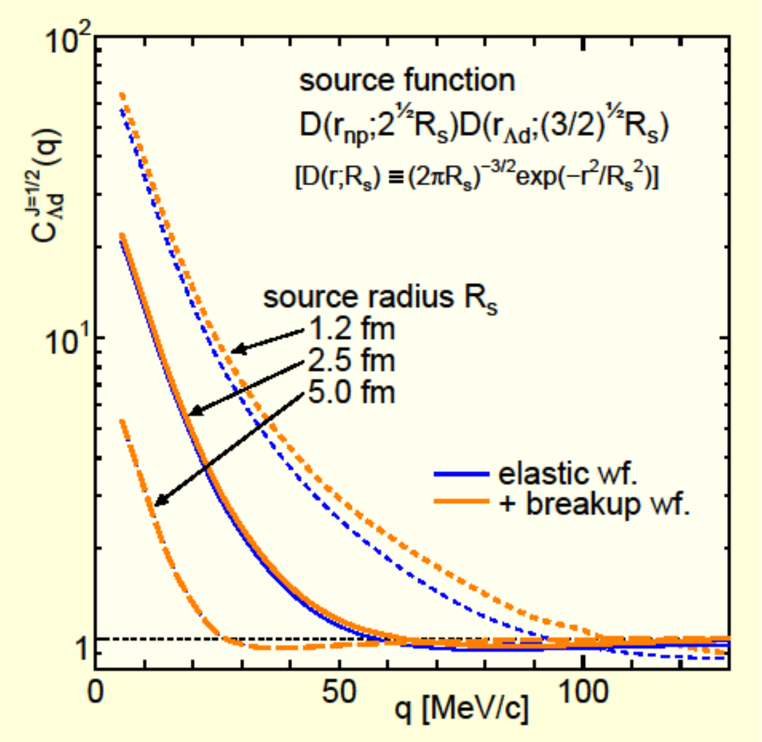

log scale